A Two-stage Stochastic Programming Approach for CRNA Scheduling with Handovers

Abhishrut Sinha
Department of Systems Science and Industrial Engineering, State University of New York, Binghamton

Ankit Bansal
Department of Systems Science and Industrial Engineering, State University of New York, Binghamton

Osman Ozaltin
Edward P. Fitts Department of Industrial and Systems Engineering, North Carolina State University

Michael Russell
Department of Anesthesiology, West Virginia University School of Medicine

We present a two-stage stochastic integer program for assigning Certified Registered Nurse Anesthetists (CRNAs) to Operating Rooms (ORs) under surgery duration uncertainty. The proposed model captures the trade-offs between CRNA staffing levels, CRNA handovers and under-staffing in the ORs. Since the stochastic program includes binary variables in both stages, we present an Integer L-shaped Algorithm to solve the model that incorporates LP Benders Cuts in addition to the standard *no-good* cuts. To further accelerate convergence, we (a) strengthen these LP Benders Cuts by tightening the second-stage formulation with valid inequalities that describe the convex hull of a binary set defined by a subset of the second-stage constraints, and (b) impose supervalid equalities that eliminate feasible second-stage solutions while retaining a subset of optimal solutions. An extensive computational study, based on the data from a tertiary medical center, reveals that our proposed solution approach efficiently solves realistic problem instances to 0.01-optimality, underscoring the effectiveness of the proposed valid inequalities and supervalid equalities. Additionally, through sensitivity analysis, we provide insights into the trade-offs between CRNA staffing levels, CRNA handovers and under-staffing.

Key words: CRNA Scheduling, Handovers, Two-Stage Stochastic Integer Program, Integer L-shaped Algorithm, Valid Inequalities, Supervalid Equalities

History:

1. Introduction

Medical errors are detrimental to patients' health and impose high costs on healthcare providers through punitive charges and litigation. A significant portion of these errors stems from communication failures (Kazemian et al. 2014). Transfer of care between providers, also known as handovers, is a major source of such failures and lower care quality, as critical details can be lost during the transition (Boet et al. 2020, Saager et al. 2014).

In this paper, we focus on intraoperative handovers between Certified Registered Nurse Anesthetists (CRNAs) transferring a patient's anesthesia care during surgery. These handovers primarily occur at shift ends, but they can also be scheduled during a shift to satisfy staffing requirements. Vital information about the patient's overall health, anesthetic plan, medications, airway management, fluid balance, surgical progress, and potential complications is communicated between CRNAs. Ideally, this exchange should be structured and comprehensive to ensure quality of care. However, time pressure and high-stress operating room (OR) settings increase the risk of incomplete or inaccurate communication, while even small omissions can lead to serious patient harm, including adverse drug reactions or delayed recognition of complications.

Although intraoperative CRNA handovers may be necessary during long surgeries due to shift changes, they should be avoided whenever possible to reduce the likelihood of communication breakdowns. This can be achieved, for example, if CRNAs work overtime. However, as daily shifts of CRNAs usually exceed 8 hours, working overtime may increase fatigue and lack of concentration, which can eventually increase the risk of medical errors (Bae 2021, Bae and Fabry 2014). Furthermore, overtime hours of CRNAs are limited by regulatory guidelines or union rules (Bae and Yoon 2014, Mobasher et al. 2011). Scheduling CRNAs on overlapping shifts with different start and end times may also reduce handovers. Then, CRNAs who have recently started their shifts can be assigned to longer surgical cases as their available shift time is more likely to encompass the full duration of the procedure.

CRNA staffing decisions are generally made at three levels (Hans et al. 2011). At the strategic level, anesthesiology departments set the size of their CRNA pool and the shift schedules. These decisions are revisited over a several-month horizon. At the tactical level, roughly four to six weeks before the day of surgery, CRNAs are rostered onto these shifts. At the operational level, once the daily surgery schedule is finalized, departments determine how many rostered CRNAs to call for duty on each shift and assign them to the surgeries scheduled for that day. We consider the operational-level problem, taking the CRNAs available on each shift and the surgery schedule as input.

We propose a two-stage stochastic integer program (SIP) for assigning CRNAs to ORs, and demonstrate its application using data from a tertiary medical center in the eastern United States. The proposed model, referred to as Stochastic CRNA Scheduling with Handovers (SCSH), captures the trade-offs between handovers and staffing while accounting for

uncertainty in surgery durations. Given the daily surgery schedules in ORs, the first-stage decisions determine the number of CRNAs to be called for a set of (overlapping) shifts with different start and end times. In the second stage, CRNAs are assigned to ORs during their shifts. The objective function minimizes the total cost of CRNA staffing, as well as the expected costs associated with CRNA handovers and under-staffing. The majority of existing nurse scheduling models in the literature focus on using overtime to mitigate workload uncertainty without accounting for handovers. A limited set of studies that consider handovers typically do so in deterministic settings or assume that handovers have no impact on the quality of care. Our model can be easily extended to consider overtime.

SCSH is a two-stage stochastic program with binary variables in both stages, and can be solved using the Integer L-shaped Algorithm (Laporte and Louveaux 1993). The feasibility and optimality cuts of the Integer L-shaped Algorithm, however, tend to be weak and result in slow convergence. Therefore, they are usually augmented with LP Benders Cuts (Angulo et al. 2016). The effectiveness of LP Benders Cuts, and consequently the convergence of the Integer L-shaped Algorithm, can be further improved by tightening the second-stage formulation. Motivated by this observation, we derive a set of valid inequalities that characterize the convex hull of the feasible region defined by the nurse assignment and handover constraints in the second stage of SCSH. Furthermore, we derive supervalid equalities, which reduce the number of feasible second-stage solutions while retaining a subset of the optimal solutions. Specifically, we establish that there exists an optimal second-stage solution in which handovers occur only at shift ends. Based on this result, the proposed equalities restrict handovers to shift ends without eliminating all optimal solutions. Our computational results show that the proposed valid inequalities and supervalid equalities substantially accelerate the convergence of the Integer L-shaped Algorithm.

The proposed valid inequalities are broadly applicable to rescheduling problems that account for service (or job) transfers between servers. Such problems arise in preemptive scheduling, where activities are interrupted and executed on a different resource when they are at risk of becoming tardy (Kirti et al. 2024), or resumed later to improve the makespan (Salvadori and Agnetis 2025, Buddhakulsomsiri and Kim 2006). The proposed valid inequalities can also strengthen formulations of reactive scheduling problems, in which

jobs affected by a server failure are reassigned to alternative servers (Kutanoglu and Sabuncuoglu 2001, Zhang et al. 2021). There are no valid inequalities proposed for these problems in the literature. The proposed supervalid equalities apply to shift-based settings in which continuity of service is valued and jobs must be transferred when a server goes off duty.

The remainder of the paper is organized as follows. Section 2 provides a review of the relevant literature. Section 3 presents the model formulation, and Section 4 describes our solution methodology. Section 5 details the proposed valid inequalities and supervalid equalities. Section 6 presents the computational experiments and managerial insights. Section 7 concludes the paper.

2. Literature Review

This paper involves both modeling and methodological advancements. Section 2.1 reviews the literature on nurse scheduling and handover processes, while Section 2.2 examines existing approaches for solving two-stage SIPs. Finally, Section 2.3 summarizes our main contributions.

2.1. Nurse Scheduling and Handovers

The literature on nurse scheduling in ORs is divided into two main categories: studies that integrate nurse scheduling with surgery scheduling (Breuer et al. 2020, Guo et al. 2016, Latorre-Núñez et al. 2016, Xiang et al. 2015) and those that concentrate exclusively on nurse scheduling for a given surgery schedule (Di Martinelly and Meskens 2017, Lim et al. 2016, Guo et al. 2014, Mobasher et al. 2011). Among these, some consider uncertainty in surgery durations (Breuer et al. 2020, Guo et al. 2014, Latorre-Núñez et al. 2016) while others solve a deterministic problem. Rath et al. (2017) and Tsang et al. (2025) present models that integrate surgery and anesthesiologist scheduling under uncertainty in surgery durations. These studies, however, do not consider handovers between providers and use overtime to mitigate the impact of uncertainty. We focus on the allocation of CRNAs to ORs for a given surgery-to-OR allocations and start times. We account for uncertainty in surgery durations and consider handovers at the end of CRNA shifts rather than overtime. The proposed model can be easily adapted to consider overtime, as we demonstrate.

The literature on handovers in scheduling problems within healthcare delivery systems in general is also limited. Kazemian et al. (2014) propose an integer programming approach

for designing shift schedules of medical trainees with the objective of minimizing handovers, while Smalley et al. (2015) present a mixed-integer programming model for physician scheduling that seeks to reduce handovers between physicians. Both of these papers address deterministic problems in non-surgical settings. Sun et al. (2023) tackle a medium-term, tactical-level anesthesiologist scheduling problem spanning multiple weeks. They develop optimization models to design shifts and assign anesthesiologists to them, accounting for uncertainties in clinical demand. In contrast, we address the operational-level CRNA scheduling problem for a given set of shifts. Sun et al. (2023) permit handovers between anesthesiologists; however, unlike our paper, their approach does not aim to reduce or limit the number of handovers.

2.2. Solution Methods for Two-Stage SIPs

A substantial body of research exists on solution methods for two-stage SIPs with integer variables in both stages (Küçükyavuz and Sen 2017). The literature can be broadly categorized into two main groups. The first group focuses on convexifying the second-stage problem by adding valid inequalities, either iteratively (Gade et al. 2014, Zhang and Kucukyavuz 2014, Sen and Higle 2005) or in a single step (Bansal et al. 2018, Kim and Mehrotra 2015). These methods enable the use of L-shaped Algorithm for solving SIPs with integer second-stage variables; however, the convexification process may be computationally intensive. The second category addresses SIPs with binary first-stage variables using the Integer L-shaped Algorithm (Laporte and Louveaux 1993, Angulo et al. 2016). This approach follows a decomposition framework in which no-good-type feasibility and optimality cuts are iteratively added to the Master Problem. In this paper, we integrate the strengths of both approaches. Specifically, we propose an Integer L-shaped Algorithm for SCSH that, in addition to the traditional no-good cuts, incorporates stronger LP Benders Cuts derived from a tighter second-stage formulation.

2.3. Contributions

The main contributions of this paper are as follows:

i. We formulate a two-stage SIP to assign CRNAs to ORs across overlapping shifts. The proposed model captures the trade-offs between CRNA staffing and handover costs under uncertainty in surgery durations. It is broadly applicable to shift-based multi-period scheduling environments in which handovers and under-staffing arise, conditions that are common in healthcare and in several other industries.

ii. We tighten the formulation of the second-stage problem in SCSH by a set of valid inequalities, which define the convex hull of the nurse assignment and handover constraints. These inequalities are generally applicable to multi-period scheduling problems involving preemptive or reactive task transfers across servers. We further derive supervalid equalities that eliminate every feasible second-stage solution in which a handover occurs before the end of the on-duty CRNA's shift, while retaining a subset of the optimal solutions. These equalities also extend to shift-based settings, in which interchangeable servers transfer jobs when they go off duty.

iii. We present an Integer L-shaped Algorithm, in which we augment the traditional no-good cuts with stronger LP Benders Cuts derived from the second-stage problem after incorporating the proposed valid inequalities and supervalid equalities. Our computational experiments show that these strengthened LP Benders Cuts substantially improve the convergence of the Integer L-shaped Algorithm.

iv. We demonstrate the applicability of SCSH using historical data from a large tertiary care hospital in the eastern United States. The computational results indicate that SCSH can help anesthesiology departments determine appropriate CRNA staffing levels by balancing trade-offs among staffing costs, handovers, and under-staffing, while accounting for uncertainty in surgery durations. When handover costs are lower than staffing costs, the optimal solution recommends calling CRNAs on shorter shifts to reduce understaffing, though with more handovers. In contrast, when handover costs are relatively high, the model recommends calling more CRNAs on longer shifts, resulting in fewer handovers but more understaffing.

3. Model Formulation

Each CRNA works on a single shift, and there are multiple shifts with different start and end times. These shifts may overlap in the time periods they cover. The first-stage problem selects CRNAs to be called for each shift. This decision can be made in advance of the day of surgery, as soon as the surgery schedule becomes available. The second-stage problem assigns CRNAs to ORs during their shifts across different scenarios of surgery-time realizations. The model minimizes the total cost of CRNA staffing, as well as the expected total cost of handovers and under-staffing.

Let S be the set of shifts, J the set of ORs, and T the set of time periods. Let c_s^f denote the cost of a CRNA on shift s, c^h the cost of a handover, and c^u the per-period cost of CRNA

under-staffing in an OR. Furthermore, let I be the set of CRNAs and $i_d \notin I$ be the index for a "dummy" CRNA, which is assigned to an OR when a regular CRNA is not available, representing under-staffing. The"dummy" CRNA serves as a placeholder for coverage gaps, defined as OR-periods with an active surgery but no available on-duty CRNA. Each such period incurs an under-staffing cost of c^u. Thus, in our modeling framework, the dummy CRNA is not associated with a shift, is not part of the first-stage staffing decision, and may be assigned to several ORs in the same period. Operationally, these under-staffed periods are covered by float CRNAs drawn from outside the scheduled pool.

Let $I_s \subseteq I$ denote the set of CRNAs working shift s, satisfying $I_{s_1} \cap I_{s_2} = \emptyset$ for all $s_1 \neq s_2 \in S$ and $\cup_{s\in S} I_s = I$. Let z_{st} be a binary parameter which equals 1 if shift s covers period t, and 0 otherwise. Let Ω be a finite set of scenarios representing the uncertainty in surgery durations, and p_ω the probability of scenario $\omega \in \Omega$. Binary parameter $\alpha_{jt}(\omega)$ equals 1 if there is an active surgery in OR j in time period t under scenario ω and 0, otherwise. Lastly, let $J_t(\omega) \subseteq J$ be the subset of ORs with an ongoing active surgery in periods t and $t+1$ under scenario ω.

The first-stage binary variable r_i takes the value 1 if CRNA i is called for duty and 0 otherwise. The second-stage binary variable $x_{ijt}(\omega)$ equals 1 if CRNA i is assigned to OR j in time period t under scenario ω, and 0 otherwise. If $x_{i_d jt}(\omega) = 1$, then CRNA under-staffing occurs in OR j during time period t. The binary variable $w_{it}(\omega)$ is equal to 1 if there is a handover from CRNA i at the end of time period t under scenario ω, and 0 otherwise. Finally, binary variable $\bar{w}_{it}(\omega)$ is equal to 1 if a handover occurs from dummy CRNA to a regular CRNA i at the end of time period t under scenario ω, and 0 otherwise. Table 1 summarizes the notation. Note that the first-stage variable r_i is defined for each CRNA because capturing handovers in the second stage requires tracking whether the same CRNA is assigned to an OR in periods t and $t+1$. This necessitates assigning individual CRNAs to ORs, and only those CRNAs called for duty in the first-stage are available in the second-stage.

We use boldface lowercase letters to denote vectors and boldface uppercase letters to represent matrices. The two-stage SIP is given by:

$$(\texttt{SCSH}) \quad v^* = \text{Min} \sum_{s\in S} \sum_{i\in I_s} c_s^f r_i + \mathcal{Q}(\mathbf{r}) \tag{1a}$$

$$\text{s.t. } r_{i_1} \geq r_{i_2} \qquad \forall s \in S,\ i_1, i_2 \in I_s :\ i_1 < i_2 \tag{1b}$$

$$\mathbf{r} \in \mathbb{B}^{|I|}. \tag{1c}$$

Table 1 Description of Notations

Sets and Parameters	
I	set of CRNAs
I_s	set of CRNAs working shift s
J	set of ORs
T	set of time periods
S	set of CRNA shifts
Ω	set of all scenarios
c_s^f	cost of calling a CRNA for shift s
c^h	cost of a handover
c^u	per-period cost of CRNA under-staffing in an OR
z_{st}	binary parameter equal to 1 if shift s covers period t, 0 otherwise
p_ω	probability of scenario ω
$J_t(\omega)$	subset of ORs with same surgery active in periods t and $t+1$ under scenario ω
$\alpha_{jt}(\omega)$	1 if there is an active surgery in OR j in time period t under scenario ω, 0 otherwise
Indices	
i	index of CRNA, $i \in I$
i_d	index of the dummy CRNA, $i_d \notin I$
j	index of OR, $j \in J$
t	index of time period, $t \in T$
s	index of shift, $s \in S$
ω	index of scenario, $\omega \in \Omega$
First-stage decision variables	
r_i	1 if CRNA i is called for duty, 0 otherwise
Second-stage decision variables	
$x_{ijt}(\omega)$	1 if CRNA i is allocated to OR j in time period t under scenario ω, 0 otherwise
$w_{it}(\omega)$	1 if a handover occurs from regular CRNA i to any other CRNA at the end of time period t under scenario ω, 0 otherwise
$\bar{w}_{it}(\omega)$	1 if a handover occurs from a dummy CRNA to regular CRNA i at the end of time period t under scenario ω, 0 otherwise

Constraint (1b) is a symmetry-breaking constraint that ensures CRNAs in each shift are selected in increasing order of their indices. The objective function (1a) minimizes the CRNA staffing cost along with the expected total cost of handovers and under-staffing $\mathcal{Q}(\mathbf{r}) \coloneqq \mathbb{E}_\omega Q(\omega, \mathbf{r}) = \sum_{\omega\in\Omega} p_\omega Q(\omega, \mathbf{r})$, where

$$(SS_{\mathbf{r},\omega}) \quad Q(\omega,\mathbf{r}) = \text{Min} \sum_{i\in I}\sum_{t\in T} c^h w_{it}(\omega) + \sum_{i\in I}\sum_{t\in T} c^h \bar{w}_{it}(\omega) + \sum_{j\in J}\sum_{t\in T} c^u x_{i_d jt}(\omega) \tag{2a}$$

$$\text{s.t.} \sum_{j\in J} x_{ijt}(\omega) \le r_i z_{st} \qquad \forall i \in I_s, s \in S, t \in T, \tag{2b}$$

$$w_{it}(\omega) \ge x_{ijt}(\omega) - x_{ij(t+1)}(\omega) \qquad \forall i \in I, j \in J_t(\omega), t \in T \setminus \{|T|\}, \tag{2c}$$

$$\bar{w}_{it}(\omega) \ge x_{i_d jt}(\omega) + x_{ij(t+1)}(\omega) - 1 \qquad \forall i \in I, j \in J_t(\omega), t \in T \setminus \{|T|\}, \tag{2d}$$

$$x_{i_d jt}(\omega) + \sum_{i\in I} x_{ijt}(\omega) = \alpha_{jt}(\omega) \qquad \forall j \in J, t \in T, \tag{2e}$$

$$\mathbf{x}(\omega) \in \mathbb{B}^{(|I|+1)\times|J|\times|T|}, \ \ \mathbf{w}(\omega), \bar{\mathbf{w}}(\omega) \in \mathbb{B}^{(|I|)\times(|T|-1)}. \tag{2f}$$

Constraint (2b) ensures that each CRNA is assigned to at most one OR in each time period. This constraint also guarantees that CRNAs are assigned to an OR in time period t only if they are scheduled for duty and their shift covers that period, thereby accounting for overlapping CRNA shifts. Constraint (2c) captures handovers from CRNA i at the end of period t. In particular, if CRNA i is assigned to OR $j \in J_t(\omega)$ in period t ($x_{ijt}(\omega) = 1$) but is not assigned to that OR in $t+1$ ($x_{ij,t+1}(\omega) = 0$), then $w_{it}(\omega) = 1$, indicating a handover from CRNA i in period t under scenario ω. There can be at most one handover from CRNA $i \in I$ in a period because (2b) restricts each CRNA i to at most one OR in any period.

Constraint (2c) cannot capture handovers from the dummy CRNA because the dummy CRNA may be assigned to multiple under-staffed ORs in the same time period. As a result, applying (2c) to a dummy CRNA would underestimate the number of handovers from the dummy CRNA to regular CRNAs at the end of each time period. Therefore, we capture these handovers through (2d). Specifically, when the dummy CRNA is assigned to OR j in time period t ($x_{i_djt}(\omega) = 1$) under scenario ω and a regular CRNA $i \in I$ is assigned to the same OR j in time period $t+1$ ($x_{ij(t+1)}(\omega) = 1$), then a handover occurs from the dummy CRNA to regular CRNA i at the end of time period t, which is recorded by setting $\bar{w}_{it}(\omega) = 1$ in (2d). Moreover, since each regular CRNA $i \in I$ is assigned to at most one OR per time period, $\bar{w}_{it}(\omega)$ can be at most 1.

Constraint (2e) ensures that a CRNA (regular or dummy) is assigned to ORs for every time period with an active surgery. The objective function (2a) minimizes the total cost of handover and CRNA under-staffing. Handovers from the dummy CRNA to a regular CRNA involve transferring care from a *float* CRNA to a regular one; hence, it constitutes an actual exchange in the responsibility of care and is therefore penalized in the objective function. SCSH has complete recourse because assigning the dummy CRNA to all ORs in all time periods by setting $x_{i_djt}(\omega) = \alpha_{jt}(\omega) \ \ \forall j \in J, \ t \in T$ in the second-stage is a feasible solution.

The proposed model captures the trade-offs between CRNA staffing and handover costs under uncertainty in surgery durations. It accommodates nurse (worker) shifts and surgery (job) schedules with heterogeneous start and end times, making it broadly applicable to shift-based multi-period scheduling environments in which handovers and under-staffing arise, conditions that are common across many medical institutions and in several other industries. Although we assume each CRNA works on a single shift on a given day, that is, $I_{s_1} \cap I_{s_2} = \emptyset$ for all $s_1 \neq s_2 \in S$, SCSH can be easily modified to handle situations where a

CRNA is available for multiple shifts. For example, if CRNA $i \in I_{s_1} \cap I_{s_2}$, we can replace i with two distinct indices, i_1 and i_2, where $i_1 \in I_{s_1}$ and $i_2 \in I_{s_2}$, and then add the constraint $r_{i_1} + r_{i_2} \leq 1$ to the first-stage problem to prevent calling CRNA i for two different shifts. Lastly, we can extend SCSH to consider CRNA overtime by tracking the last time period in which CRNAs are allocated to an OR after their shift ends, as shown in Appendix D. These extensions will not impact the methodological approaches that we propose for the efficient solution of SCSH.

4. Integer L-shaped Algorithm for SCSH

The L-shaped Algorithm can be applied to SCSH after relaxing the integrality of the second-stage binary variables. The algorithm generates LP Benders Cuts whenever an integer first-stage solution is identified within a Branch-and-Bound framework (see Appendix A for more details). The optimal objective value of the relaxed problem provides a lower bound for SCSH. Furthermore, the first-stage solution $\mathbf{r}$ obtained from the L-shaped Algorithm can be used to evaluate $\mathcal{Q}(\mathbf{r})$ and derive an upper bound. However, this approach does not ensure global optimality.

The Integer L-shaped Algorithm (ILS) can be applied to obtain the global optimal solution to SCSH. This method can also be also executed within a Branch-and-Bound framework, where the algorithm is initialized with the following master problem:

$$(\mathcal{M}) \quad \text{Min} \sum_{s \in S} \sum_{i \in I_s} c_s^f r_i + \sum_{\omega \in \Omega} p_\omega \theta_\omega \tag{3a}$$

$$\text{s.t. } r_{i_1} \geq r_{i_2} \qquad \forall s \in S,\ i_1, i_2 \in I_s :\ i_1 < i_2 \tag{3b}$$

$$\theta_\omega \geq 0 \qquad \forall \omega \in \Omega \tag{3c}$$

$$\mathbf{r} \in \mathbb{B}^{|I|} \tag{3d}$$

where θ_ω is an auxiliary variable representing the second-stage cost under scenario ω. Subsequently, for each integer solution $(\bar{\boldsymbol{\theta}}, \bar{\mathbf{r}})$ encountered during the Branch-and-Bound algorithm, and for every scenario ω where $\bar{\theta}_\omega < Q(\omega, \bar{\mathbf{r}})$, the following Integer Optimality Cut is added to $\mathcal{M}$:

$$\theta_\omega \geq Q(\omega, \bar{\mathbf{r}}) \left(\sum_{i \in S(\bar{\mathbf{r}})} r_i - \sum_{i \notin S(\bar{\mathbf{r}})} r_i - |S(\bar{\mathbf{r}})| \right) + Q(\omega, \bar{\mathbf{r}}), \tag{4}$$

where $S(\bar{\mathbf{r}}) = \{i \in I | \bar{r}_i = 1\}$. This cut eliminates the solution $(\bar{\boldsymbol{\theta}}, \bar{\mathbf{r}})$ if $\bar{\theta}_\omega < Q(\omega, \bar{\mathbf{r}})$ for scenario ω. The right-hand side of (4) equals $Q(\omega, \bar{\mathbf{r}})$ at $\mathbf{r} = \bar{\mathbf{r}}$, yielding the tightest possible

underestimation of θ_ω at $\bar{\mathbf{r}}$. However, if $\mathbf{r} \neq \bar{\mathbf{r}}$, (4) becomes redundant since its right-hand side takes on a non-positive value. As a result, `Integer Optimality Cuts` contribute little to strengthening the lower bounds within the `Branch-and-Bound` algorithm, which in turn slows the convergence of `ILS`. The performance can potentially be improved by generating `LP Benders Cuts` in addition to the `Integer Optimality Cuts`. This approach, referred to as `ILS-L`, first attempts to eliminate an integer solution using `LP Benders Cuts` derived from the LP relaxations of the second-stage problems. If no `LP Benders Cuts` are found, `Integer Optimality Cuts` are added to $\mathcal{M}$. Algorithm 1 presents the corresponding optimality cut subroutine.

Algorithm 1 Optimality Cut Subroutine

Input: $(\bar{\mathbf{r}}, [\bar{\theta}_\omega]_{\omega\in\Omega})$
for $\omega \in \Omega$ **do**
  Obtain $Q^l(\omega, \bar{\mathbf{r}})$, objective value of the LP relaxation of $SS_{\mathbf{r},\omega}$
  if $Q^l(\omega, \bar{\mathbf{r}}) > \bar{\theta}_\omega$ **then**
    Add `LP Benders Cut` (13) (stated in Appendix A) to $\mathcal{M}$. ▷ `Step 1`
  end if
end for
if No `LP Benders Cuts` are added in Step 1 **then**
  $S(\bar{\mathbf{r}}) \leftarrow \{i : \bar{r}_i = 1\}$
  for $\omega \in \Omega$ **do**
    Obtain $Q(\omega, \bar{\mathbf{r}})$
    if $Q(\omega, \bar{\mathbf{r}}) > \bar{\theta}_\omega$ **then**
      Add `Integer Optimality Cut` (4) to $\mathcal{M}$ ▷ `Step 2`
    end if
  end for
end if

We apply `ILS-L` to solve `SCSH`. To accelerate the convergence, we modify the formulation of the second-stage problem $SS_{\mathbf{r},\omega}$ in two ways. First, we derive valid inequalities to tighten the formulation of second-stage problem $SS_{\mathbf{r},\omega}$ and strengthen the `LP Benders Cuts`. We demonstrate that the proposed valid inequalities characterize the convex hull

of the assignment and handover constraints defined for each CRNA $i \in I$, $t \in T \setminus \{|T|\}$ and ORs in the set J_t. Second, we derive supervalid equalities that eliminate feasible solutions of $SS_{\mathbf{r},\omega}$ while retaining a subset of optimal solutions. Our computational experiments in Section 6.1 show that the proposed valid inequalities and supervalid equalities complement each other in accelerating the convergence of ILS-L.

5. Valid Inequalities and Supervalid Equalities for the Second-Stage Formulation

In this section, we omit the scenario index ω for clarity of the presentation. For a given first-stage solution $\mathbf{r}$, let $\mathcal{P}(\mathbf{r})$ be the set of feasible second-stage solutions. We modify the formulation of the second-stage problem in two ways. Section 5.1 presents valid inequalities for $\mathcal{P}(\mathbf{r})$ while Section 5.2 presents supervalid equalities for $SS_{\mathbf{r},\omega}$. Proofs of all the propositions are stated in Appendix B.

5.1. Valid Inequalities for $SS_{\mathbf{r},\omega}$

Proposition 1 presents a set of valid inequalities for $\mathcal{P}(\mathbf{r})$.

PROPOSITION 1. *For $i \in I$ and $t \in T \setminus \{|T|\}$, the inequalities*

$$w_{it} \geq \sum_{j \in \bar{J}} \left(x_{ijt} - x_{ij(t+1)}\right) \qquad \forall \bar{J} \subseteq J_t \tag{5}$$

are valid for $\mathcal{P}(\mathbf{r})$.

Valid inequalities in (5) capture a handover from CRNA i at the end of time period t if that CRNA is assigned to an OR in $\bar{J} \subseteq J_t$ during time period t but not assigned an OR in the same subset in period $t+1$. The summation over ORs on the right-hand side of (5) is valid because CRNA i can be assigned to at most one OR in $\bar{J}$ in each period t and $t+1$. Thus, the term inside the sum can equal 1 for at most one OR in $\bar{J} \subseteq J_t$, and (5) generalizes (2c) by accounting for handovers within each subset of ORs. Example 1 demonstrates that inequality (5) cuts off fractional solutions that are feasible to (2c).

EXAMPLE 1. Consider an instance of $SS_{\mathbf{r},\omega}$ with $I = \{1\}, T = \{1,2\}, r_1 = 1, J = J_1 = \{1,2\}$ and $\alpha_{11} = \alpha_{21} = \alpha_{12} = \alpha_{22} = 1$. The solution $w_{11} = 0.5, \bar{w}_{11} = 0, x_{111} = 0.5, x_{121} = 0.5, x_{112} = 0, x_{122} = 0, x_{i_d 11} = 0.5, x_{i_d 21} = 0.5, x_{i_d 12} = 1, x_{i_d 22} = 1$ is feasible to the LP relaxation of $SS_{\mathbf{r},\omega}$ but violates the following valid inequality (5) for $t = 1$ with $\bar{J} = J_t$:

$$\underbrace{w_{11}}_{0.5} \geq \underbrace{x_{111} + x_{121}}_{1} - \underbrace{x_{112} - x_{122}}_{0}.$$

For $i \in I$, $t \in T \setminus \{|T|\}$, let $\mathcal{Q}_{it}$ be a binary set given by:

$$\mathcal{Q}_{it} = \begin{cases} w_{it} \geq x_{ijt} - x_{ij(t+1)} & \forall j \in J_t, \\ \sum_{j \in J_t} x_{ijt} \leq 1,\ \sum_{j \in J_t} x_{ij(t+1)} \leq 1, & \\ w_{it} \in \{0,1\}, x_{ijt}, x_{ij(t+1)} \in \{0,1\} & \forall j \in J_t \end{cases} \tag{6}$$

Constraints (6) restrict the assignment of CRNA i to at most one OR in J_t during the periods t and $t+1$, and determine whether a handover occurs from CRNA i at the end of period t. This constraint structure commonly appears in multi-period preemptive or reactive scheduling problems, where the transfer of tasks across resources is tracked (Salvadori and Agnetis 2025, Buddhakulsomsiri and Kim 2006).

Let $\tilde{\mathcal{Q}}_{it}$ denote the linear relaxation of $\mathcal{Q}_{it}$. Additionally, let the projection operator be defined as $\text{Proj}_{(x)}\,\mathcal{X} = \{\, x : \exists y \text{ such that } (x,y) \in \mathcal{X} \,\}$. The main theoretical result of this paper pertains to showing that adding valid inequalities (5) to $\tilde{\mathcal{Q}}_{it}$ characterizes the convex hull of $\mathcal{Q}_{it}$, which is denoted by $\text{conv}(\mathcal{Q}_{it})$. The proof is achieved in two steps. First, in Proposition 2, we use a disjunctive programming technique to derive a polyhedron $\mathcal{V}_{it}$ in an extended variable space whose projection onto the space of $(w_{it}, \mathbf{x}_{it}, \mathbf{x}_{i(t+1)})$ variables gives $\text{conv}(\mathcal{Q}_{it})$. Then, in Proposition 3, we utilize *Hoffman's Circulation Theorem* (Hoffman 1976) to show that the $\text{Proj}_{(w_{it}, \mathbf{x}_{it}, \mathbf{x}_{i(t+1)})}\,\mathcal{V}_{it}$ is characterized by $\tilde{\mathcal{Q}}_{it}$ and inequalities in (5).

PROPOSITION 2. *For a given $i \in I$, $t \in T \setminus \{|T|\}$, define the auxiliary variables x^1_{ijt} and $x^1_{ij(t+1)}$ $\forall j \in J_t$. Furthermore, let $\mathcal{V}_{it}$ be the polyhedron given by*

$$x_{ijt} - x_{ij(t+1)} \leq x^1_{ijt} - x^1_{ij(t+1)} \leq w_{it} \qquad \forall j \in J_t, \tag{7a}$$

$$-1 + w_{it} + \sum_{j \in J_t} x_{ijt} \leq \sum_{j \in J_t} x^1_{ijt} \leq w_{it}, \tag{7b}$$

$$-1 + w_{it} + \sum_{j \in J_t} x_{ij(t+1)} \leq \sum_{j \in J_t} x^1_{ij(t+1)} \leq w_{it}, \tag{7c}$$

$$0 \leq x^1_{ijt} \leq x_{ijt} \qquad \forall j \in J_t, \tag{7d}$$

$$0 \leq x^1_{ij(t+1)} \leq x_{ij(t+1)} \qquad \forall j \in J_t. \tag{7e}$$

Then, $\text{conv}(\mathcal{Q}_{it}) = \text{Proj}_{(w_{it}, \mathbf{x}_{it}, \mathbf{x}_{i(t+1)})}\,\mathcal{V}_{it}$.

Proposition 3 presents the projection of $\mathcal{V}_{it}$ onto $(w_{it}, \mathbf{x}_{it}, \mathbf{x}_{i(t+1)})$ variable space.

PROPOSITION 3. $\text{Proj}_{(w_{it},\mathbf{x}_{it},\mathbf{x}_{i(t+1)})}\mathcal{V}_{it}$ *is given by the following set of constraints:*

$$\tilde{\mathcal{Q}}_{it}^{L} = \begin{cases} (w_{it},\mathbf{x}_{it},\mathbf{x}_{i(t+1)}) \in \tilde{\mathcal{Q}}_{it}, \\ w_{it} \geq \sum_{j\in\bar{J}} \left(x_{ijt} - x_{ij(t+1)}\right) \quad \forall \bar{J} \subseteq J_t, |\bar{J}| \geq 2. \end{cases} \tag{8}$$

Using Propositions 2 and 3, we obtain the following corollary, which shows that adding valid inequalities (5) to $\tilde{\mathcal{Q}}_{it}$ yields $\text{conv}(\mathcal{Q}_{it})$.

COROLLARY 1. $\text{conv}(\mathcal{Q}_{it}) = \tilde{\mathcal{Q}}_{it}^{L}$

Corollary 1 suggests that including valid inequalities (5) to $SS_{\mathbf{r},\omega}$ can lead to a tighter formulation of $SS_{\mathbf{r},\omega}$. Therefore, generating `LP Benders Cuts` based on this formulation can accelerate the convergence of `ILS-L`. For each $i \in I$, $t \in T \setminus |T|$, the number of valid inequalities (5) are exponential in $|J_t|$. The following proposition presents a polynomial size reformulation for these valid inequalities.

PROPOSITION 4. *For $i \in I$, $t \in T \setminus \{|T|\}$, valid inequalities* (5) *and $w_{it} \geq 0$ can be reformulated as:*

$$w_{it} \geq \sum_{j\in J_t} \beta_{ijt} \tag{9a}$$

$$\beta_{ijt} \geq x_{ijt} - x_{ij(t+1)} \qquad \forall j \in J_t, \tag{9b}$$

$$\beta_{ijt} \geq 0 \qquad \forall j \in J_t. \tag{9c}$$

We implement valid inequalities (5) through (9) in our computational experiments.

5.2. Supervalid Equalities for $SS_{\mathbf{r},\omega}$

In the following proposition, we introduce equalities for $SS_{\mathbf{r},\omega}$ that restrict its feasible region while retaining a subset of the optimal solutions. Equalities with this property are known as *supervalid* (Israeli and Wood 2002, Lozano and Smith 2017).

PROPOSITION 5. *Let $T_s^e = \max\{t \in T : z_{st} = 1\}$ denote the last time period covered by shift s. The equalities*

$$w_{it} = 0 \qquad \forall i \in I_s, t \in T \setminus \{|T|, T_s^e\}, s \in S \tag{10}$$

are supervalid for $SS_{\mathbf{r},\omega}$.

Proposition 5 states that there exists an optimal second-stage solution in which every handover from a CRNA in I_s occurs at the end of their shift. The proof relies on considering an optimal second-stage solution where there is a handover from a CRNA before the end of their shift, and constructing from it a feasible solution in which this handover is relocated to the end of the shift, without increasing either the number of handovers or the number of under-staffed periods.

Imposing (10) results in a smaller feasible region for $SS_{\mathbf{r},\omega}$, and hence reduces the time required to solve each scenario subproblem. Since ILS-L solves $|\Omega|$ scenario subproblems at every integer feasible first-stage solution encountered in the Branch-and-Bound tree, these savings accumulate over the course of the algorithm and accelerates its convergence, as we show in Section 6.1.

Like the valid inequalities of Section 5.1, equalities (10) exploit only structural features common to a broader class of problems. They are therefore broadly applicable to shift-based multi-period scheduling environments in which a pool of identical servers is organized into shifts and jobs must be transferred when a server goes off duty, conditions that arise in service systems where continuity of service is valued.

6. Computational Experiments

Our computational experiments are based on data from a tertiary medical hospital in the eastern United States. The dataset consists of 14,883 surgeries across 24 specialties, spanning a period of 353 working days. For each specialty, Table 6 in Appendix C provides the mean and standard deviation of surgery durations, along with the percentage share of total surgeries attributed to each specialty. We assume that the surgery duration for each specialty follows a log-normal distribution (Neyshabouri and Berg 2017).

We consider four shifts of differing lengths; the periods covered by each shift are reported in Table 7 in Appendix C. The planning horizon is divided into $|T|= 56$ equal time intervals of 15 minutes each. We experiment with the surgery schedules of three different days. More details about each scheduled surgery, including its specialty, planned start time, and the assigned OR, are provided in Appendix C.

Let $c^r = 200$ denote the hourly cost of a CRNA. We set the cost of calling a shift s CRNA (c^f_s) equal to the product of c^r and the length of shift s. Our experiments only require that c^f_s increase with shift length; the formulation accommodates any cost structure, including

one in which longer shifts are disproportionately more expensive. While the hourly cost of CRNAs is known in practice, estimating the costs of under-staffing and handovers can be challenging due to their downstream effects on clinic operations and patient health outcomes. Consequently, we specify these cost parameters relative to CRNA staffing cost, informed by our medical collaborator's acceptable levels of expected handovers and under-staffing in the resulting schedules. Subsequently, we set handover cost (c^h) and per-period CRNA under-staffing cost (c^u) using the ratios $\psi = \frac{c^h}{c^r}$, and $\chi = \frac{c^u}{c^r}$. We consider three values of $\psi = 30, 40, 50$ and three values of $\chi = 5, 10, 20$. Note that extreme values of these parameters lead to trivial solutions. If ψ or χ is set too high, placing excessive emphasis on avoiding handovers or under-staffing, nearly all CRNAs would be called for duty. Conversely, if these parameters are too low, few or no CRNAs would be scheduled, resulting in a large number of handovers or under-staffed periods. We design a full factorial experiment over the values of ψ and χ, resulting in 9 different *cases* for each $|\Omega|$. We consider $|\Omega| = 500$ and 1000 scenarios, each with equal probability. Furthermore, we generate three random instances for each of the three days per case, that is, 9 different instances per case, for a total of 81 instances for each $|\Omega|$. We perform all computations using Python 3.9.12 and Gurobi 11.0.2 on a machine with a 14-core Intel Xeon 2.60GHz processor and 128GB of RAM.

The remainder of this section is organized as follows: Section 6.1 compares different algorithmic approaches for solving SCSH, Section 6.2 examines the value of incorporating stochasticity in surgery durations, and Section 6.3 provides a sensitivity analysis by varying the handover and under-staffing costs to offer managerial insights.

6.1. Computational Performance Analysis

In this section, we compare the performance of the following five methods to solve SCSH:

1. ILS-L: ILS-L with no valid inequalities or supervalid equalities added to $SS_{\mathbf{r},\omega}$.
2. ILS-L$_{(5)}$: ILS-L with valid inequalities (5) added to $SS_{\mathbf{r},\omega}$.
3. ILS-L$_{(10)}$: ILS-L with supervalid equalities (10) added to $SS_{\mathbf{r},\omega}$.
4. ILS-L$_{(5,10)}$: ILS-L with valid inequalities (5), supervalid equalities (10) added to $SS_{\mathbf{r},\omega}$.
5. ExF: Extensive Form solved using Gurobi 11.0.2.

For all instances, each method is run with a time limit of 3600 seconds and a target optimality gap of 1%. The runtimes of the ILS-L variants may exceed the 3600-second limit on certain instances. This occurs because if the algorithm enters the optimality cut subroutine near the time limit, it is allowed to finish that subroutine before termination,

resulting in the total runtime exceeding 3600 seconds. For each of the 9 cases defined by ψ and χ, Tables 11 and 12 in Appendix E report the average (maximum) % optimality gaps and runtimes (in seconds) of the four ILS-L variants with $|\Omega|= 500$ and 1000 scenarios, respectively. ExF does not solve any instance to within a 1% optimality gap for either value of $|\Omega|$, and its average optimality gap exceeds 75% in every case. We therefore exclude it from the comparison below.

Figure 1 compares the four ILS-L variants on the 81 instances generated for each value of $|\Omega|$. For each method, the curve shows the percentage of instances solved to 1%-optimality as a function of the runtime. As shown in Figure 1, all three strengthened variants solve more instances to 1% optimality than ILS-L, and ILS-L$_{(5,10)}$ performs best overall. When $|\Omega|= 500$, ILS-L$_{(5,10)}$ obtains 0.01-optimal solutions for all instances, while ILS-L obtains them for 83% of instances within 3600 seconds. The difference is more pronounced when $|\Omega|= 1000$. ILS-L$_{(5,10)}$ still obtains 0.01-optimal solutions for all instances, whereas ILS-L does so for only 35%. The ILS-L$_{(5)}$ and ILS-L$_{(10)}$ variants fall in between, with ILS-L$_{(5)}$ performing better than ILS-L$_{(10)}$.

While Figure 1 aggregates the results over all instances, Table 2 reports, for each case, the average (maximum) percentage reduction in runtime achieved by each strengthened variant relative to ILS-L. For each instance, the percentage reduction for variant $A \in \{\text{ILS-L}_{(5)}, \text{ILS-L}_{(10)}, \text{ILS-L}_{(5,10)}\}$ is calculated as $\frac{\text{Runtime}^{\text{ILS-L}} - \text{Runtime}^{A}}{\text{Runtime}^{\text{ILS-L}}} \times 100$. Tables 3 and 4 report the following average (maximum) Branch-and-Bound statistics for $|\Omega|= 500$ and $|\Omega|= 1000$, respectively: the number of calls to Algorithm 1, the numbers of LP Benders Cuts and Integer Optimality Cuts generated, the number of nodes explored, and the total runtime (in seconds). As shown in Table 2, ILS-L$_{(5,10)}$ achieves the largest overall speedup, reducing the average runtime relative to ILS-L by at least 47.5% across the nine cases for $|\Omega|= 500$ and by at least 33.4% for $|\Omega|= 1000$. The valid inequalities (5) and the supervalid equalities (10) are also individually helpful, each reducing the average runtime of ILS-L in every case.

Comparisons of ILS-L$_{(5)}$ and ILS-L$_{(10)}$ with ILS-L isolate the distinct mechanisms through which the valid inequalities (5) and the supervalid equalities (10), respectively, improve the computational performance of ILS-L. The primary benefit of ILS-L$_{(5)}$ is a substantial reduction in the size of the Branch-and-Bound tree. Relative to ILS-L, ILS-L$_{(5)}$ reduces the average runtime by at least 38.2% across the nine cases when $|\Omega|= 500$ and

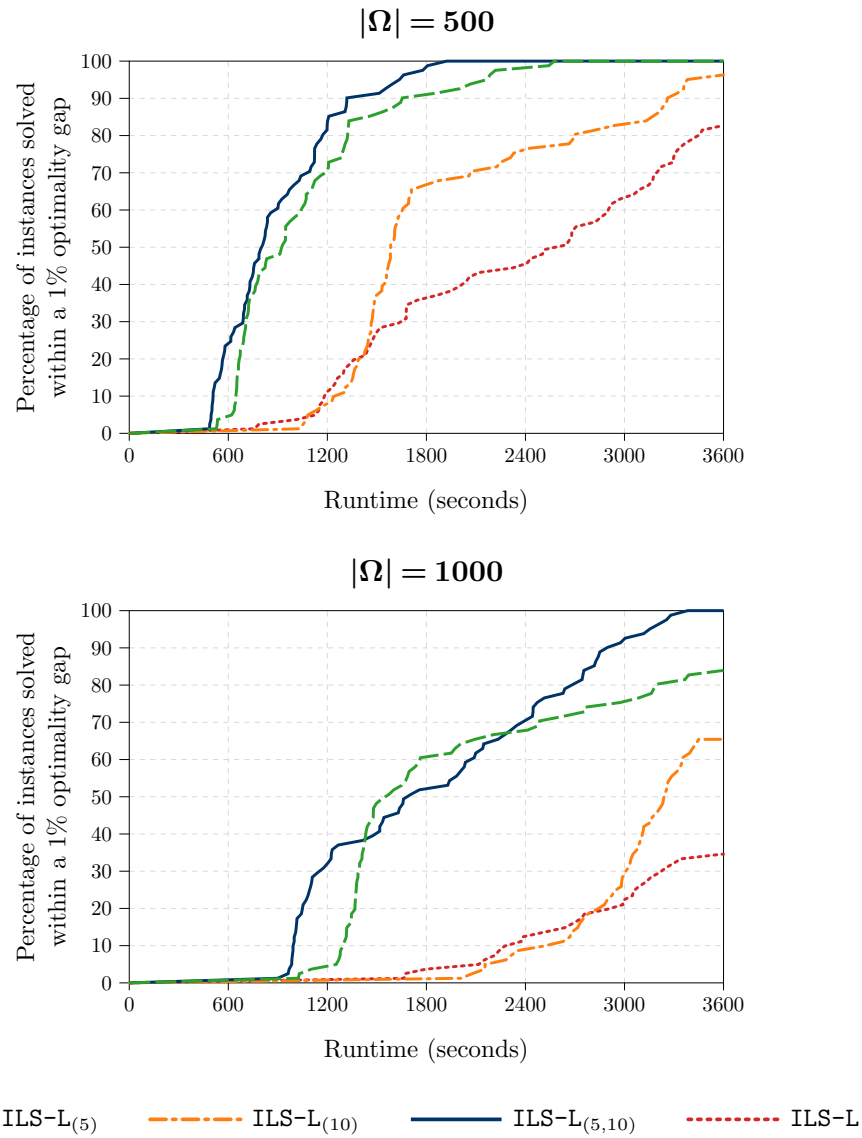


Figure 1 **Percentage of instances solved to within a 1% optimality gap over time, for** $|\Omega| = 500$ **(top) and** $|\Omega| = 1000$ **(bottom).** ExF **is omitted: it solves no instance to within a 1% optimality gap in 3600 seconds.**

Table 2 Average (max) reduction in runtime (%) relative to ILS-L.

Case	ψ—χ	$\|\Omega\| = 500$			$\|\Omega\| = 1000$		
		ILS-L$_{(5)}$	ILS-L$_{(10)}$	ILS-L$_{(5,10)}$	ILS-L$_{(5)}$	ILS-L$_{(10)}$	ILS-L$_{(5,10)}$
1	30—5	47.76 (81.10)	19.49 (54.81)	56.46 (84.19)	36.40 (63.39)	1.30 (15.05)	39.86 (71.69)
2	30—10	41.88 (77.61)	13.50 (47.64)	57.48 (82.77)	36.63 (65.85)	3.97 (18.47)	46.77 (74.36)
3	30—20	38.23 (80.45)	0.34 (42.66)	48.73 (79.37)	32.60 (55.84)	0.93 (29.45)	40.17 (68.23)
4	40—5	45.71 (73.58)	12.92 (51.38)	49.65 (81.98)	37.53 (68.54)	1.55 (36.42)	43.30 (76.71)
5	40—10	59.16 (80.24)	22.08 (52.32)	66.35 (84.61)	48.31 (68.67)	5.79 (19.54)	46.85 (75.95)
6	40—20	54.12 (69.26)	4.26 (36.41)	57.63 (76.32)	35.61 (67.15)	3.76 (41.39)	45.12 (75.05)
7	50—5	47.78 (62.16)	17.53 (43.84)	47.47 (71.24)	36.82 (62.96)	0.86 (26.65)	33.42 (69.22)
8	50—10	64.57 (79.76)	21.38 (57.29)	68.61 (84.03)	41.75 (67.25)	8.45 (32.49)	47.82 (74.96)
9	50—20	67.69 (75.78)	18.43 (45.24)	67.45 (81.20)	45.71 (70.79)	12.98 (26.97)	55.69 (77.78)

by at least 32.6% when $|\Omega| = 1000$. This improvement is consistent with the integrality gap closed by (5): tightening the relaxation of $SS_{\mathbf{r},\omega}$ produces stronger `LP Benders Cuts`, which in turn yield stronger lower bounds and reduce the amount of `Branch-and-Bound` search required. The statistics in Tables 3 and 4 support this explanation. For $|\Omega| = 500$, `ILS-L`$_{(5)}$ requires fewer than half as many calls to Algorithm 1 as `ILS-L` (12.3 versus 29.6) and explores approximately one-tenth as many nodes (4.7 versus 50.3). A similar pattern emerges for $|\Omega| = 1000$: the number of calls to Algorithm 1 decreases from 22.8 to 12.1, while the number of nodes explored decreases from 24.7 to 4.9.

In contrast, `ILS-L`$_{(10)}$ improves computational performance primarily by reducing the effort required per call to Algorithm 1. Recall that `ILS-L` solves $|\Omega|$ scenario subproblems at every integer-feasible solution encountered during the `Branch-and-Bound` search. Consequently, even modest reductions in scenario subproblem solution times can lead to substantial cumulative savings. For $|\Omega| = 500$, `ILS-L`$_{(10)}$ makes nearly the same average number of calls to Algorithm 1 as `ILS-L` (30.2 versus 29.6), while reducing average runtime by approximately 20%, from 2452 to 1952 seconds. For $|\Omega| = 1000$, the average runtime decreases by approximately 6.9%, from 3483 to 3244 seconds, despite an increase in the average number of calls to Algorithm 1 from 22.8 to 26.3. Interestingly, `ILS-L`$_{(10)}$ also explores more `Branch-and-Bound` nodes than `ILS-L` for both $|\Omega| = 500$ (53.2 versus 50.3) and $|\Omega| = 1000$ (38.1 versus 24.7). These observations suggest that the reduced computational effort per call to Algorithm 1 allows `ILS-L`$_{(10)}$ to explore more of the `Branch-and-Bound` tree within the time limit, contributing to its improved performance in solving instances to within 1% of optimality, as shown in Figure 1.

Overall, the two enhancements improve `ILS-L` through complementary mechanisms: (5) facilitates more effective pruning of the `Branch-and-Bound` nodes by strengthening the `LP Benders Cuts`, whereas (10) reduces the computational effort required to process each node. By combining these benefits, `ILS-L`$_{(5,10)}$ achieves the largest overall runtime reductions.

6.2. Comparison with the `Mean Value Solution`

To assess the impact of modeling uncertainty in surgery durations, Table 5 compares the best solution obtained from `ILS-L`$_{(5,10)}$ (`Stochastic Solution`) in Section 6.1 with the `Mean Value Solution` (Birge and Louveaux 2011) for $|\Omega| = 500$. Column 3 of Table 5 reports the average Value of the Stochastic Solution (VSS), computed as $\frac{MV-UB}{MV} \times 100$,

Table 3 Average (max) `Branch-and-Bound` statistics, $|\Omega|=500$.

	ILS-L	ILS-L$_{(5)}$	ILS-L$_{(10)}$	ILS-L$_{(5,10)}$
Calls to Algorithm 1	29.6 (39)	12.3 (22)	30.2 (45)	12.1 (20)
`LP Benders Cuts`	1665 (3401)	482 (1784)	1705 (3549)	486 (1316)
`Integer Optimality Cuts`	6144 (11339)	727 (2265)	6356 (12817)	702 (2095)
Nodes explored	50.3 (75)	4.7 (30)	53.2 (88)	4.2 (20)
Runtime (s)	2452 (3910)	1055 (2575)	1952 (3899)	902 (1923)

Note. Averages and maximums are reported over all 81 instances. For instances not solved within the time limit, the statistics are those at termination.

Table 4 Average (max) `Branch-and-Bound` statistics, $|\Omega|=1000$.

	ILS-L	ILS-L$_{(5)}$	ILS-L$_{(10)}$	ILS-L$_{(5,10)}$
Calls to Algorithm 1	22.8 (35)	12.1 (18)	26.3 (37)	12.7 (24)
`LP Benders Cuts`	2261 (5385)	983 (2224)	3121 (6344)	1118 (4087)
`Integer Optimality Cuts`	8426 (13909)	1445 (4070)	10063 (16391)	1437 (3656)
Nodes explored	24.7 (51)	4.9 (21)	38.1 (66)	6.1 (28)
Runtime (s)	3483 (4699)	2122 (4196)	3244 (4310)	1866 (3382)

Note. Averages and maximums are reported over all 81 instances. For instances not solved within the time limit, the statistics are those at termination.

where UB and MV denote the objective value evaluated at the `Stochastic Solution` and `Mean Value Solution`, respectively. Columns 4–10 report the average percentage reductions in various performance measures under `Stochastic Solution` relative to `Mean Value Solution`. Specifically, Columns 4–6 present these reductions for the expected number of handovers (`HO`), expected number of under-staffed periods (`US`), and first-stage staffing cost (`SC`), respectively. Columns 7–10 present the corresponding reductions in the number of shift-k `CRNA`s called for duty ($\texttt{S}_\texttt{k}$), for $k=1,2,3,4$ (see Table 7). The percentage reduction is calculated as $\kappa_l = \frac{l_{MV}-l_{SS}}{l_{MV}} \times 100$, where l_{MV} and l_{SS} denote the values of performance measure l under `Mean Value Solution` and `Stochastic Solution`, respectively. A positive κ_l indicates a reduction under `Stochastic Solution`, whereas a negative value indicates an increase. Results for $|\Omega|=1000$ are presented in Appendix E.

As shown in Column 3 of Table 5, incorporating uncertainty in surgery durations leads to a substantial reduction in the objective value. These savings are primarily driven by lower expected under-staffing and/or handovers under `Stochastic Solution` relative to `Mean Value Solution`, as observed in Columns 4 and 5. This effect arises because, as shown in Columns 7 and 8, `Stochastic Solution` tends to replace Shift 1 `CRNA`s in the `Mean Value Solution` with longer Shift 2 `CRNA`s. This substitution increases coverage and reduces under-staffed periods and/or handovers, and the resulting expected cost savings outweigh the higher staffing costs observed in Column 6. Moreover, this preference for

Table 5 Comparison of Stochastic Solution and Mean Value Solution ($|\Omega|= 500$).

Case	ψ—χ	VSS	κ_{HO}	κ_{US}	κ_{SC}	κ_{S_1}	κ_{S_2}	κ_{S_3}	κ_{S_4}
1	30—5	2.71	-12.69	9.58	-2.07	38.89	-34.44	0.00	0.00
2	30—10	4.93	2.84	10.43	-2.33	44.44	-40.00	0.00	0.00
3	30—20	6.26	10.09	8.92	-2.54	55.56	-51.11	0.00	0.00
4	40—5	2.45	-13.85	8.19	-2.33	44.44	-40.00	0.00	0.00
5	40—10	4.76	-2.45	10.66	-2.33	44.44	-40.00	0.00	0.00
6	40—20	6.44	8.63	9.30	-2.54	55.56	-51.11	0.00	0.00
7	50—5	2.36	-7.91	7.06	-2.07	38.89	-34.44	0.00	0.00
8	50—10	4.52	-6.43	10.27	-2.33	44.44	-40.00	0.00	0.00
9	50—20	6.48	5.66	10.75	-4.39	33.33	-40.00	0.00	0.00

Shift 2 over Shift 1 CRNAs becomes more pronounced at higher values of the under-staffing cost parameter χ, leading to significant reductions in both expected under-staffed periods and handovers. These observations remain consistent when $|\Omega|= 1000$.

6.3. Sensitivity Analysis

In this section, we examine how the expected number of handovers, the expected number of under-staffed time periods, and the number of CRNAs assigned to each shift vary in response to changes in handover cost and under-staffing costs. The results also verify that SCSH captures the trade-offs between staffing cost, handovers, and under-staffing as intended. To better understand these trade-offs, we allow up to 10 CRNAs per shift and consider six values of the handover cost parameter, $\psi \in \{20, 30, 40, 50, 60, 70\}$, along with six values of the per-period under-staffing cost parameter, $\chi \in \{2.5, 5, 10, 20, 30, 40\}$. For these parameter settings, we consider the best solution obtained from ILS-L$_{(5,10)}$. Results are averaged over three randomly generated instances of the SCSH corresponding to the Day 3 surgery schedule with $|\Omega|= 500$. As in Section 6.1, ILS-L$_{(5,10)}$ is solved with a 3600-second time limit and a target optimality gap of 1%.

Figure 2a, for $\chi = 10$, shows the variation in the expected number of handovers and the expected number of under-staffed time periods as the handover cost parameter ψ increases from 20 to 70. Similarly, Figure 2b depicts, for the same value of χ and increasing ψ, the changes in the number of CRNAs assigned per shift and the total cost of CRNAs. Figure 3a and Figure 3b present the same variations for $\psi = 40$ and increasing per-period under-staffing cost parameter χ from 2.5 to 40.

In Figure 2b, the number of CRNAs called for each shift remains the same as ψ increases from 20 to 40. However, we observe in Figure 2a that the average number of handovers decreases while the average number of under-staffed time periods increases as expected.

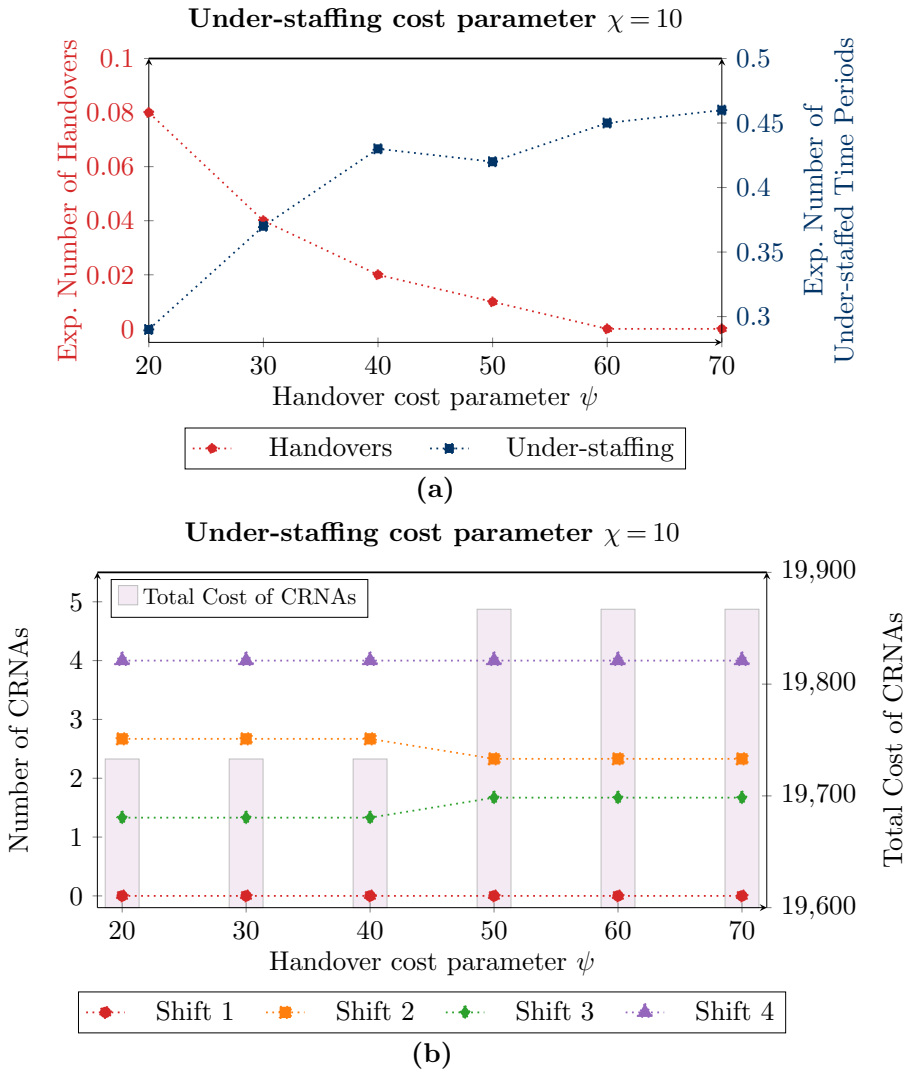


Figure 2 **Analysis of the trade-off between handovers and CRNA staffing.**

Thus, at a higher handover cost, some surgeries are not assigned any CRNAs because the shifts of all the available CRNAs end during these surgeries, and incurring under-staffing instead of handover is more cost-effective. However, as ψ increases to 50, a Shift 3 CRNA is called in-place of a Shift 2 CRNA. As Shift 3 CRNA can cover a larger number of time periods, both the average number of handovers and the average number of under-staffed time periods decrease at the expense of increased staffing cost.

In Figure 3a, the expected number of handovers increases while the expected number of under-staffed time periods decreases as the per-period under-staffing cost parameter χ increases from 2.5 to 20. This is because both handovers and additional CRNA coverage are used to reduce under-staffing. Additionally, as illustrated in Figure 3b, the total cost of

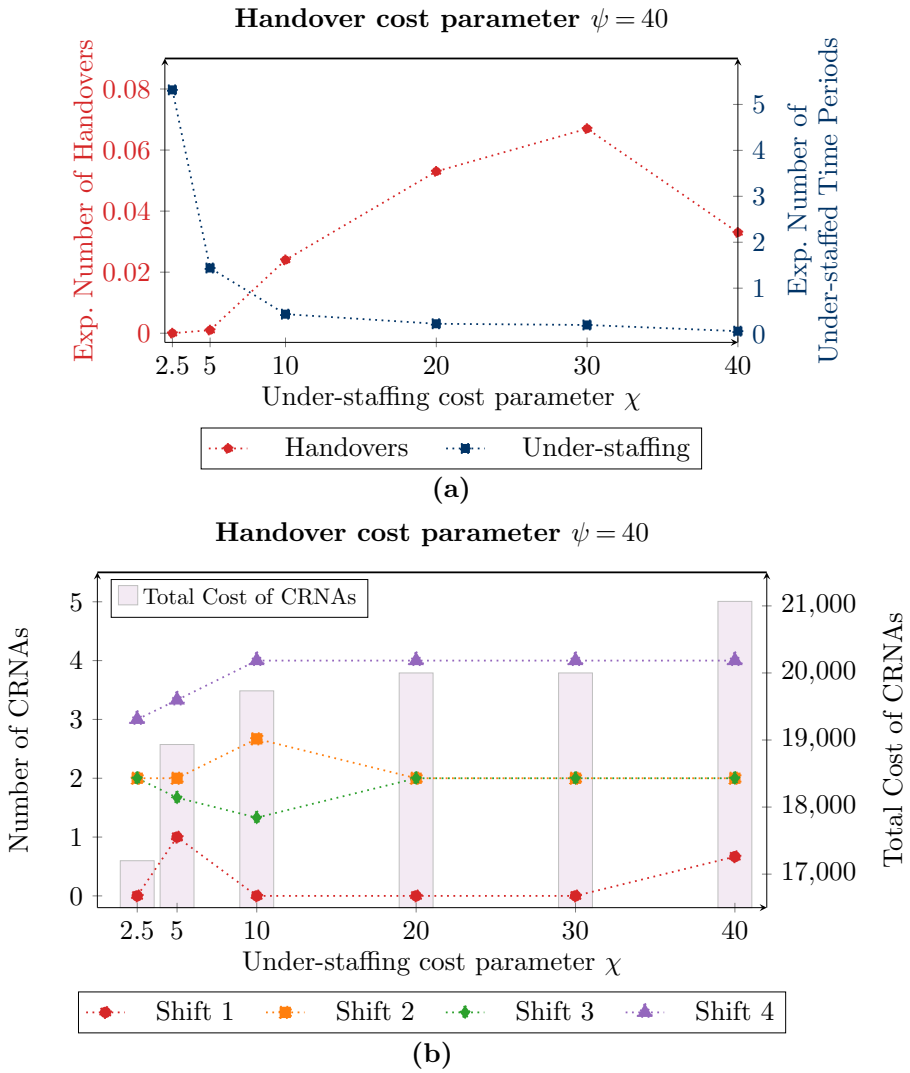


Figure 3 **Analysis of the trade-off between under-staffing and CRNA staffing.**

CRNAs increases as χ increases from 2.5 to 20. For example, as χ increases from 5 to 10, Shift 2 and Shift 4 CRNAs are called in-place of Shift 1 and Shift 3 CRNAs. The model favors calling more nurses on longer shifts to cover surgeries scheduled later in the day, where the effects of accumulated duration uncertainty are most pronounced. Lastly, when χ increases to 40, calling an additional Shift 1 CRNA becomes cost-effective, providing sufficient CRNA coverage to reduce both the number of handovers and under-staffed time periods.

7. Conclusion

We propose SCSH, a two-stage stochastic program to staff CRNA shifts. Specifically, SCSH captures the trade-offs between staffing cost, handovers, and under-staffing while accounting for uncertainty in surgery durations. Given the daily surgery schedules in ORs, it deter-

mines, in the first stage, the number of CRNAs to be called for each shift. In the second stage, on-duty CRNAs are assigned to ORs over the time periods within their shifts. The proposed model captures the trade-offs between CRNA staffing and handover costs under uncertainty in surgery durations. It is broadly applicable to shift-based multi-period scheduling environments in which handovers and under-staffing arise, conditions that are common across many medical institutions and in several other industries. Additionally, our formulation can be extended to incorporate overtime without affecting the proposed solution approach.

We present an Integer L-shaped Algorithm for solving SCSH that incorporates LP Benders Cuts in addition to the standard *no-good* cuts. To further accelerate convergence, we strengthen these LP Benders Cuts by tightening the second-stage formulation. To this end, we derive valid inequalities for the second-stage problem. We demonstrate that the proposed valid inequalities define the convex hull of the nurse assignment and handover constraints. These inequalities are broadly applicable to multi-period scheduling problems that involve preemptive or reactive transfer of tasks across resources. We further derive supervalid equalities that eliminate feasible solutions from the second-stage problem while retaining a subset of optimal solutions. Our computational experiments demonstrate that the proposed valid inequalities and supervalid equalities are highly effective, leading to substantial improvements in the convergence of the Integer L-shaped Algorithm.

This paper demonstrates that explicitly incorporating uncertainty in surgery durations while optimizing the mix of CRNAs across shifts yields meaningful performance improvements over mean-value solutions, without significantly increasing CRNA costs. The resulting stochastic solutions reduce one or both cost components associated with handovers and under-staffing, depending on the trade-offs implied by their relative costs. From an operational perspective, the model reveals how uncertainty compounds over the course of the day, increasing the likelihood of coverage gaps and handovers in later periods. Mitigating these downstream effects may require increasing CRNA hours or opening additional ORs. Overall, the proposed framework provides a principled basis for evaluating and comparing alternative mitigation strategies. These insights and proposed methods are broadly applicable to multi-period scheduling problems involving service transfers across resources. Future research could extend SCSH to jointly optimize both surgery schedules and CRNA assignments. Another promising direction is to incorporate add-on surgeries, which are added to the OR schedule at the last minute, into the modeling framework.

References

Angulo G, Ahmed S, Dey SS (2016) Improving the integer L-shaped method. *INFORMS Journal on Computing* 28(3):483–499.

Bae SH (2021) Relationships between comprehensive characteristics of nurse work schedules and adverse patient outcomes: a systematic literature review. *Journal of Clinical Nursing* 30(15-16):2202–2221.

Bae SH, Fabry D (2014) Assessing the relationships between nurse work hours/overtime and nurse and patient outcomes: systematic literature review. *Nursing Outlook* 62(2):138–156.

Bae SH, Yoon J (2014) Impact of states' nurse work hour regulations on overtime practices and work hours among registered nurses. *Health Services Research* 49(5):1638–1658.

Bansal M, Huang KL, Mehrotra S (2018) Tight second stage formulations in two-stage stochastic mixed integer programs. *SIAM Journal on Optimization* 28(1):788–819.

Birge JR, Louveaux F (2011) *Introduction to Stochastic Programming* (Springer Science & Business Media).

Boet S, Djokhdem H, Leir SA, Théberge I, Mansour F, Etherington C (2020) Association of intraoperative anaesthesia handovers with patient morbidity and mortality: a systematic review and meta-analysis. *British Journal of Anaesthesia* 125(4):605–613.

Breuer DJ, Lahrichi N, Clark DE, Benneyan JC (2020) Robust combined operating room planning and personnel scheduling under uncertainty. *Operations Research for Health Care* 27:100276.

Buddhakulsomsiri J, Kim DS (2006) Properties of multi-mode resource-constrained project scheduling problems with resource vacations and activity splitting. *European Journal of Operational Research* 175(1):279–295.

Conforti M, Cornuéjols G, Zambelli G, Conforti M, Cornuéjols G, Zambelli G (2014) *Integer Programming* (Springer).

Di Martinelly C, Meskens N (2017) A bi-objective integrated approach to building surgical teams and nurse schedule rosters to maximise surgical team affinities and minimise nurses' idle time. *International Journal of Production Economics* 191:323–334.

Gade D, Küçükyavuz S, Sen S (2014) Decomposition algorithms with parametric gomory cuts for two-stage stochastic integer programs. *Mathematical Programming* 144(1):39–64.

Guo M, Wu S, Li B, Rong Y (2014) Maximizing the efficiency of use of nurses under uncertain surgery durations: a case study. *Computers & Industrial Engineering* 78:313–319.

Guo M, Wu S, Li B, Song J, Rong Y (2016) Integrated scheduling of elective surgeries and surgical nurses for operating room suites. *Flexible Services and Manufacturing Journal* 28:166–181.

Hans EW, Van Houdenhoven M, Hulshof PJ (2011) A framework for healthcare planning and control. *Handbook of healthcare system scheduling*, 303–320 (Springer).

Hoffman AJ (1976) Total unimodularity and combinatorial theorems. *Linear Algebra and its Applications* 13(1-2):103–108.

Israeli E, Wood RK (2002) Shortest-path network interdiction. *Networks: An International Journal* 40(2):97–111.

Kazemian P, Dong Y, Rohleder TR, Helm JE, Van Oyen MP (2014) An ip-based healthcare provider shift design approach to minimize patient handoffs. *Health Care Management Science* 17:1–14.

Kim K, Mehrotra S (2015) A two-stage stochastic integer programming approach to integrated staffing and scheduling with application to nurse management. *Operations Research* 63(6):1431–1451.

Kirti M, Maurya AK, Yadav RS (2024) Fault-tolerant allocation of deadline-constrained tasks through preemptive migration in heterogeneous cloud environments. *Cluster Computing* 27(8):11427–11454.

Küçükyavuz S, Sen S (2017) An introduction to two-stage stochastic mixed-integer programming. *Leading Developments from INFORMS Communities*, 1–27 (INFORMS).

Kutanoglu E, Sabuncuoglu I (2001) Routing-based reactive scheduling policies for machine failures in dynamic job shops. *International Journal of Production Research* 39(14):3141–3158.

Laporte G, Louveaux FV (1993) The integer l-shaped method for stochastic integer programs with complete recourse. *Operations Research Letters* 13(3):133–142.

Latorre-Núñez G, Lüer-Villagra A, Marianov V, Obreque C, Ramis F, Neriz L (2016) Scheduling operating rooms with consideration of all resources, post anesthesia beds and emergency surgeries. *Computers & Industrial Engineering* 97:248–257.

Lim GJ, Mobasher A, Bard JF, Najjarbashi A (2016) Nurse scheduling with lunch break assignments in operating suites. *Operations Research for Health Care* 10:35–48.

Lozano L, Smith JC (2017) A value-function-based exact approach for the bilevel mixed-integer programming problem. *Operations Research* 65(3):768–786.

Mobasher A, Lim G, Bard JF, Jordan V (2011) Daily scheduling of nurses in operating suites. *IIE Transactions on Healthcare Systems Engineering* 1(4):232–246.

Neyshabouri S, Berg BP (2017) Two-stage robust optimization approach to elective surgery and downstream capacity planning. *European Journal of Operational Research* 260(1):21–40.

Rath S, Rajaram K, Mahajan A (2017) Integrated anesthesiologist and room scheduling for surgeries: Methodology and application. *Operations Research* 65(6):1460–1478.

Saager L, Hesler BD, You J, Turan A, Mascha EJ, Sessler DI, Kurz A (2014) Intraoperative transitions of anesthesia care and postoperative adverse outcomes. *Anesthesiology* 121(4):695–706.

Salvadori I, Agnetis A (2025) The impact of the number of preemptions in resource-constrained project scheduling problems with time-varying resources: computational experiments and a case study. *Annals of Operations Research* 1–30.

Sen S, Higle JL (2005) The C^3 theorem and a D^2 algorithm for large scale stochastic mixed-integer programming: Set convexification. *Mathematical Programming* 104:1–20.

Smalley HK, Keskinocak P, Vats A (2015) Physician scheduling for continuity: an application in pediatric intensive care. *Interfaces* 45(2):133–148.

Sun K, Sun M, Agrawal D, Dravenstott R, Rosinia F, Roy A (2023) Equitable anesthesiologist scheduling under demand uncertainty using multiobjective programming. *Production and Operations Management* 32(11):3699–3716.

Tsang MY, Shehadeh KS, Curtis FE, Hochman BR, Brentjens TE (2025) Stochastic optimization approaches for an operating room and anesthesiologist scheduling problem. *Operations Research* 73(3):1430–1458.

Xiang W, Yin J, Lim G (2015) A short-term operating room surgery scheduling problem integrating multiple nurses roster constraints. *Artificial Intelligence in Medicine* 63(2):91–106.

Zhang M, Kucukyavuz S (2014) Finitely convergent decomposition algorithms for two-stage stochastic pure integer programs. *SIAM Journal on Optimization* 24(4):1933–1951.

Zhang S, Tang F, Li X, Liu J, Zhang B (2021) A hybrid multi-objective approach for real-time flexible production scheduling and rescheduling under dynamic environment in industry 4.0 context. *Computers & Operations Research* 132:105267.

Appendices

Appendix A: Details of the L-shaped Algorithm

The L-shaped Algorithm to solve SCSH involves relaxing the integrality of the second-stage binary variables and solving the resulting relaxation. Let v^l be the optimal objective function value of the relaxed problem where $v^l \leq v^*$. Let $\bar{\mathbf{r}}$ be the first-stage solution obtained at the termination of the L-shaped Algorithm, then $v^u = \sum_{s\in S}\sum_{i\in I_s} c_s^f \bar{r}_i + \sum_{\omega\in\Omega} p_\omega Q(\omega, \bar{\mathbf{r}})$ given an upper bound on v^*. If $\frac{v^u - v^l}{v^u} \leq \epsilon$, then the L-shaped Algorithm yields an ϵ-optimal solution.

We implement L-shaped Algorithm for SCSH on a single Branch-and-Bound tree. We initialize the algorithm by solving the following master problem using the Branch-and-Bound algorithm:

$$(\mathcal{M}^L) \quad \text{Min} \quad \sum_{s\in S}\sum_{i\in I_s} c_s^f r_i + \sum_{\omega\in\Omega} p_\omega \theta_\omega \tag{11a}$$

$$\text{s.t.} \quad r_{i_1} \geq r_{i_2} \qquad \forall s \in S,\ \ i_1, i_2 \in I_s :\ \ i_1 < i_2 \tag{11b}$$

$$\theta_\omega \geq 0 \qquad \forall \omega \in \Omega, \tag{11c}$$

$$\mathbf{r} \in \mathbb{B}^{|I|}. \tag{11d}$$

For each integer feasible solution $(\bar{\mathbf{r}}, \bar{\boldsymbol{\theta}})$ encountered within any node of the Branch-and-Bound tree, we solve the following subproblem for each scenario $\omega \in \Omega$:

$$Q^l(\omega, \bar{\mathbf{r}}) = \text{Min} \ \sum_{i\in I}\sum_{t\in T} c^h w_{it}(\omega) + \sum_{j\in J}\sum_{t\in T} c^u x_{i_d jt}(\omega) + \sum_{i\in I}\sum_{t\in T} c^h \bar{w}_{it}(\omega) \tag{12a}$$

$$\text{s.t.} \ (\mu^1_{ijt}) \quad w_{it}(\omega) \geq x_{ijt}(\omega) - x_{ij(t+1)}(\omega) \qquad \forall i \in I, j \in J_t(\omega), t \in T \setminus \{|T|\}, \tag{12b}$$

$$(\mu^2_{ijt}) \quad \bar{w}_{it}(\omega) \geq x_{i_d jt}(\omega) + x_{ij(t+1)}(\omega) - 1 \qquad \forall i \in I, j \in J_t(\omega), t \in T \setminus \{|T|\}, \tag{12c}$$

$$(\mu^3_{ist}) \quad \sum_{j\in J} x_{ijt}(\omega) \leq \bar{r}_i z_{st} \qquad \forall i \in I_s, s \in S, t \in T, \tag{12d}$$

$$(\mu^4_{jt}) \quad \sum_{i\in I} x_{ijt}(\omega) + x_{i_d jt}(\omega) = \alpha_{jt}(\omega) \qquad \forall j \in J, t \in T, \tag{12e}$$

$$(\mu^5_{it}) \quad w_{it}(\omega) \leq 1 \qquad \forall i \in I, t \in T \setminus \{|T|\}, \tag{12f}$$

$$(\mu^6_{it}) \quad \bar{w}_{it}(\omega) \leq 1 \qquad \forall i \in I, t \in T \setminus \{|T|\}, \tag{12g}$$

$$(\mu^7_{ijt}) \quad x_{ijt}(\omega) \leq 1 \qquad \forall i \in I, j \in J, t \in T, \tag{12h}$$

$$\mathbf{w}(\omega), \bar{\mathbf{w}}(\omega), \mathbf{x}(\omega) \geq 0 \tag{12i}$$

The notation for the optimal dual solution is stated in parentheses before the constraints. For each $\omega \in \Omega$, if $Q^l(\omega, \bar{\mathbf{r}}^k) > \bar{\theta}_\omega$, the following optimality cut is added to $\mathcal{M}^L$ to exclude the solution $(\bar{\mathbf{r}}, \bar{\boldsymbol{\theta}})$:

$$\begin{aligned}\theta_\omega \geq & - \sum_{\substack{i\in I, j\in J_t(\omega),\\ t\in T\setminus\{|T|\}}} \mu^2_{ijt} + \sum_{\substack{i\in I_s,\\ s\in S, t\in T}} \mu^3_{ist} r_i z_{st} + \sum_{j\in J, t\in T} \mu^4_{jt}\alpha_{jt}(\omega) \\ & + \sum_{i\in I, t\in T\setminus\{|T|\}} \mu^5_{it} + \sum_{i\in I, t\in T\setminus\{|T|\}} \mu^6_{it} + \sum_{i\in I, j\in J, t\in T} \mu^7_{ijt}.\end{aligned} \tag{13}$$

Appendix B: Proof of Propositions

Proof of Proposition 1: Assume that for some $(\mathbf{x}^*, \mathbf{w}^*, \bar{\mathbf{w}}^*) \in \mathcal{P}(\mathbf{r})$, there exists an $i \in I$, $t \in T \setminus \{|T|\}$, and $\bar{J} \subseteq J_t$ such that:

$$w^*_{it} < \sum_{j\in\bar{J}} \left(x^*_{ijt} - x^*_{ij(t+1)}\right) \tag{14}$$

Then, from (2b) and (2f), it must be that $w^*_{it} = 0$ and $\exists j_1 \in \bar{J}$ such that $x^*_{ij_1t} = 1, x^*_{ij_1(t+1)} = 0$. In that case, however, (2c) enforces $w^*_{it} \geq 1$, which is a contradiction. □

Proof of Proposition 2: For the ease of presentation, we use x_{j1} to represent x_{ijt}, x_{j2} in place of $x_{ij(t+1)}$, and w for w_{it}. We represent $\mathcal{Q}_{it}$ as the union of two disjoint sets as $P_1 \cup P_2$, where

$$P_1 = \begin{cases} x_{j1} - x_{j2} - w \leq 0, & \forall j \in J_t, \\ \sum_{j\in J_t} x_{j1} \leq 1, & \\ \sum_{j\in J_t} x_{j2} \leq 1, & \\ x_{j1}, x_{j2} \in \{0,1\} & \forall j \in J_t, \\ w = 1. & \end{cases} \qquad P_2 = \begin{cases} x_{j1} - x_{j2} - w \leq 0, & \forall j \in J_t, \\ \sum_{j\in J_t} x_{j1} \leq 1, & \\ \sum_{j\in J_t} x_{j2} \leq 1, & \\ x_{j1}, x_{j2} \in \{0,1\} & \forall j \in J_t, \\ w = 0. & \end{cases}$$

Let $\tilde{P}_1$ and $\tilde{P}_2$ be the linear programming relaxations of P_1 and P_2, respectively. As the constraint matrices for the variables $x_{j1}, x_{j2}\ \forall j \in J_t$ are totally unimodular (TU), $\text{conv}(P_1) = \tilde{P}_1$ and $\text{conv}(P_2) = \tilde{P}_2$. Consequently, as $\tilde{P}_1$ and $\tilde{P}_2$ are bounded, $\text{conv}(\mathcal{Q}_{it}) = \text{conv}(\tilde{P}_1 \cup \tilde{P}_2)$ (Conforti et al. 2014). Furthermore, $\text{conv}(\tilde{P}_1 \cup \tilde{P}_2)$ is given by the projection of the following polyhedron onto the $(\mathbf{x_1}, \mathbf{x_2}, w)$ variable space (Conforti et al. 2014).

$$x^1_{j1} - x^1_{j2} - w^1 \leq 0, \qquad x^2_{j1} - x^2_{j2} - w^2 \leq 0, \qquad \forall j \in J_t, \tag{15a}$$

$$\sum_{j\in J_t} x^1_{j1} \le \lambda^1, \qquad \sum_{j\in J_t} x^2_{j1} \le \lambda^2, \tag{15b}$$

$$\sum_{j\in J_t} x^1_{j2} \le \lambda^1, \qquad \sum_{j\in J_t} x^2_{j2} \le \lambda^2, \tag{15c}$$

$$w^1 = \lambda^1, \qquad w^2 = 0, \tag{15d}$$

$$x^1_{j1}, x^1_{j2} \ge 0, \qquad x^2_{j1}, x^2_{j2} \ge 0, \qquad \forall j \in J_t, \tag{15e}$$

$$x^1_{j1} + x^2_{j1} = x_{j1}, \qquad \forall j \in J_t, \tag{15f}$$

$$x^1_{j2} + x^2_{j2} = x_{j2}, \qquad \forall j \in J_t, \tag{15g}$$

$$w^1 + w^2 = w, \tag{15h}$$

$$\lambda^1 + \lambda^2 = 1, \tag{15i}$$

$$0 \le \lambda^1, \lambda^2 \le 1. \tag{15j}$$

From (15d), (15f), (15g), (15h) and (15i), we get the equalities $w^1 = w$, $w^2 = 0$, $\lambda^1 = w$, $\lambda^2 = (1-w)$, $x^2_{j1} = x_{j1} - x^1_{j1}$, and $x^2_{j2} = x_{j2} - x^1_{j2}$. Substituting these equalities in the inequalities of (15) we obtain:

$$x_{j1} - x_{j2} \le x^1_{j1} - x^1_{j2} \le w \qquad \forall j \in J_t, \tag{16a}$$

$$-1 + w + \sum_{j\in J_t} x_{j1} \le \sum_{j\in J_t} x^1_{j1} \le w, \tag{16b}$$

$$-1 + w + \sum_{j\in J_t} x_{j2} \le \sum_{j\in J_t} x^1_{j2} \le w, \tag{16c}$$

$$0 \le x^1_{j1} \le x_{j1} \qquad \forall j \in J_t, \tag{16d}$$

$$0 \le x^1_{j2} \le x_{j2} \qquad \forall j \in J_t. \tag{16e}$$

Substituting $x_{j1} = x_{ijt}$, $x_{j2} = x_{ij(t+1)}$, and $w = w_{it}$ in (16), we get $\mathcal{V}_{it}$. □

Next, we state the *Hoffman's Circulation Theorem* (Hoffman 1976), which is a key component required for the proof of Proposition 3.

LEMMA 1. *Hoffman Circulation Theorem (1976): Let $G = (V, E)$ be a directed graph. Let $\ell, u : E \mapsto \mathbb{R} \cup \{\pm\infty\}$ denote the lower and upper bounds of flow on arc e. Assume that $\ell(e) \le u(e)$ for every $e \in E$. Then, there exists a feasible flow $\sigma : E \mapsto \mathbb{R}$ that satisfies (i) $\ell(e) \le \sigma(e) \le u(e)$ for every $e \in E$, and (ii) $\sum_{(a,b)\in E} \sigma(a,b) = \sum_{(b,a)\in E} \sigma(b,a)$ for all $a \in V$, if and only if*

$$\sum_{(a,b)\in\delta^+(X)} \ell(a,b) \le \sum_{(a,b)\in\delta^-(X)} u(a,b) \qquad \forall X \subseteq V \tag{17}$$

where $\delta^-(X) := \{(a,b) \in E : a \notin X, b \in X\}$ *and* $\delta^+(X) := \{(a,b) \in E : a \in X, b \notin X\}$.

A feasible flow σ that satisfies conditions (i) and (ii) specified in Lemma 1 is referred to as a *circulation*.

Proof of Proposition 3: For the ease of presentation, we use x_{j1} to represent x_{ijt}, x_{j2} in place of $x_{ij(t+1)}$, and w for w_{it}. Consider the directed graph $G(\bar{V}, \bar{E})$ shown in Figure 4 with $\sigma(a,b)$ representing the flow along the arc $(a,b) \in \bar{E}$, and $\ell(a,b)$ and $u(a,b)$ denote the lower and upper bounds, respectively, for $\sigma(a,b)$. In $G(\bar{V}, \bar{E})$, $\bar{V} = \{d_1, d_2, q\} \cup \{p_j, j \in J_t\}$, $\bar{E} = \{(d_1, p_j), \forall j \in J_t\} \cup \{(p_j, q), \forall j \in J_t\} \cup \{(p_j, d_2), \forall j \in J_t\} \cup \{(q, d_2), (d_2, d_1)\}$. Denote $\sigma(d_1, p_j)$ by x^1_{j1} $\forall j \in J_t$, $\sigma(p_j, q)$ by x^1_{j2} $\forall j \in J_t$, and let

$$\ell(a,b) = \begin{cases} 0 & a = d_1, b = p_j \ \ \forall j \in J_t \\ x_{j1} - x_{j2} & a = p_j, b = d_2 \ \ \forall j \in J_t \\ 0 & a = p_j, b = q \ \ \forall j \in J_t \\ -1 + w + \sum_{j \in J_t} x_{j2} & a = q, b = d_2 \\ -1 + w + \sum_{j \in J_t} x_{j1} & a = d_2, b = d_1 \end{cases} \qquad u(a,b) = \begin{cases} x_{j1} & a = d_1, b = p_j \ \ \forall j \in J_t \\ w & a = p_j, b = d_2 \ \ \forall j \in J_t \\ x_{j2} & a = p_j, b = q \ \ \forall j \in J_t \\ w & a = q, b = d_2 \\ w & a = d_2, b = d_1 \end{cases}$$

Applying the two conditions in Lemma 1 to $G(\bar{V}, \bar{E})$, we obtain:

$$0 \le \sigma(d_1, p_j) = x^1_{j1} \le x_{j1} \qquad \forall j \in J_t \tag{18a}$$

$$x_{j1} - x_{j2} \le \sigma(p_j, d_2) \le w \qquad \forall j \in J_t \tag{18b}$$

$$0 \le \sigma(p_j, q) = x^1_{j2} \le x_{j2} \qquad \forall j \in J_t \tag{18c}$$

$$-1 + w + \sum_{j \in J_t} x_{j2} \le \sigma(q, d_2) \le w \tag{18d}$$

$$-1 + w + \sum_{j \in J_t} x_{j1} \le \sigma(d_2, d_1) \le w \tag{18e}$$

$$\sigma(p_j, d_2) = x^1_{j1} - x^1_{j2} \qquad \forall j \in J_t \tag{18f}$$

$$\sigma(q, d_2) = \sum_{j \in J_t} x^1_{j2} \tag{18g}$$

$$\sigma(d_2, d_1) = \sum_{j \in J_t} x^1_{j1} \tag{18h}$$

In particular, (18a)-(18e) and (18f)-(18h) are obtained by applying (i) and (ii), respec-

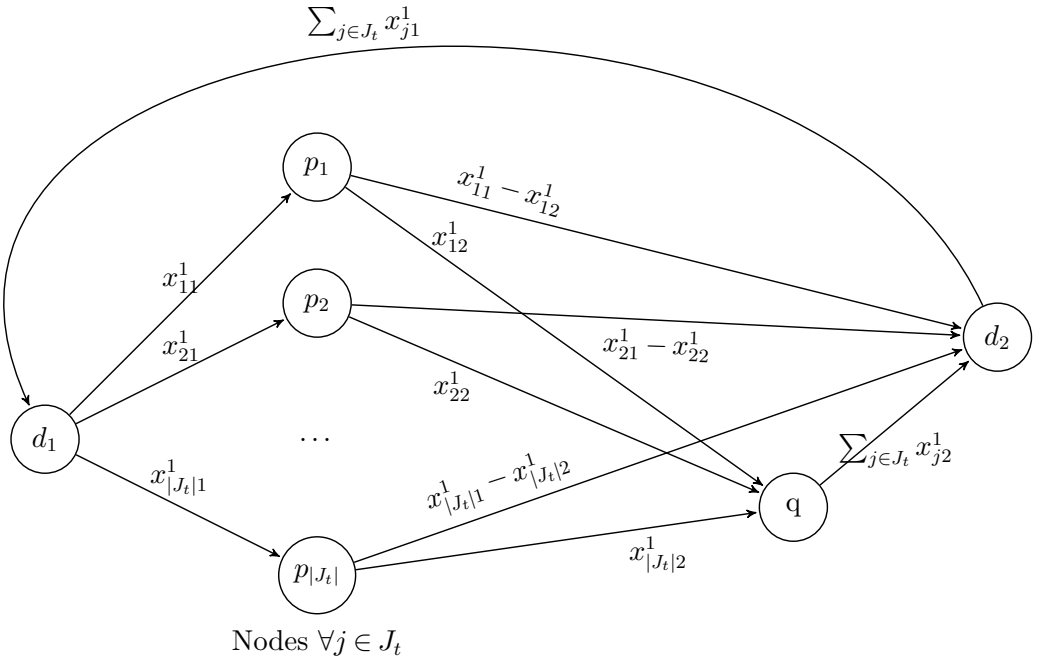


Figure 4 $G(\bar{V}, \bar{E})$ **for the Proof of Proposition 3. The labels on the arcs indicate the flow variables.**

tively. Using the equalities in (18f), (18g) and (18h) in (18b), (18d) and (18e), respectively, we get the constraint set (16) that define $\mathcal{V}_{it}$. Thus, a circulation exists on $G(\bar{V}, \bar{E})$ if and only if $\mathcal{V}_{it} \neq \emptyset$.

Next, we apply (17) to $G(\bar{V}, \bar{E})$ to derive another condition for the existence of a circulation. Let $\bar{J} \subseteq \{p_j : j \in J_t\}$. Note that $\bar{J}$ can be empty. Consider the following cases:

Case 1. $X = \{d_1, [p_j]_{j\in\bar{J}}\}$: For this case, $\delta^+(X) = \{(p_j, q)\ \ \forall j \in \bar{J}\} \cup \{(p_j, d_2)\ \ \forall j \in \bar{J}\} \cup \{(d_1, p_j)\ \ \forall j \in J_t \setminus \bar{J}\}$, $\delta^-(X) = \{(d_2, d_1)\}$. (17) $\Rightarrow$

$$\sum_{j\in\bar{J}} \ell(p_j, q) + \sum_{j\in\bar{J}} \ell(p_j, d_2) + \sum_{j\in J\setminus\bar{J}} \ell(d_1, p_j) \leq u(d_2, d_1)$$
$$\Rightarrow \sum_{j\in\bar{J}} (x_{j1} - x_{j2}) \leq w \tag{19}$$

Case 2. $X = \{[p_j]_{j\in\bar{J}}\}$: For this case, $\delta^+(X) = \{(p_j, q)\ \ \forall j \in \bar{J}\} \cup \{(p_j, d_2)\ \ \forall j \in \bar{J}\}$, $\delta^-(X) = \{(d_1, p_j)\ \ \forall j \in \bar{J}\}$. (17) $\Rightarrow$

$$\sum_{j\in\bar{J}} \ell(p_j, q) + \sum_{j\in\bar{J}} \ell(p_j, d_2) \leq \sum_{j\in\bar{J}} u(d_1, p_j)$$

$$\Rightarrow \sum_{j\in\bar{J}}(x_{j1}-x_{j2}) \leq \sum_{j\in\bar{J}} x_{j1}$$
$$\Rightarrow \sum_{j\in\bar{J}} x_{j2} \geq 0 \tag{20}$$

Case 3. $X = \{[p_j]_{j\in\bar{J}}, q\}$: For this case, $\delta^+(X) = \{(p_j, d_2)\ \forall j \in \bar{J}\} \cup (q, d_2)$, $\delta^-(X) = \{(d_1, p_j)\ \forall j \in \bar{J}\} \cup \{(p_j, q)\ \forall j \in J_t \setminus \bar{J}\}$. (17) $\Rightarrow$

$$\sum_{j\in\bar{J}} \ell(p_j, d_2) + \ell(q, d_2) \leq \sum_{j\in\bar{J}} u(d_1, p_j) + \sum_{J_t\setminus\bar{J}} u(p_j, q)$$
$$\Rightarrow \sum_{j\in\bar{J}}(x_{j1}-x_{j2}) - 1 + w + \sum_{j\in J_t} x_{j2} \leq \sum_{j\in\bar{J}} x_{j1} + \sum_{J_t\setminus\bar{J}} x_{j2}$$
$$\Rightarrow w \leq 1 \tag{21}$$

Case 4. $X = \{[p_j]_{j\in\bar{J}}, d_2\}$: For this case, $\delta^+(X) = \{(p_j, q)\ \forall j \in \bar{J}\} \cup (d_2, d_1)$, $\delta^-(X) = \{(d_1, p_j)\ \forall j \in \bar{J}\} \cup \{(p_j, d_2)\ \forall j \in J_t \setminus \bar{J}\} \cup (q, d_2)$. (17) $\Rightarrow$

$$\sum_{j\in\bar{J}} \ell(p_j, q) + \ell(d_2, d_1) \leq \sum_{j\in\bar{J}} u(d_1, p_j) + \sum_{j\in J_t\setminus\bar{J}} u(p_j, d_2) + u(q, d_2)$$
$$\Rightarrow -1 + w + \sum_{j\in J_t} x_{j1} \leq \sum_{j\in\bar{J}} x_{j1} + \sum_{j\in J_t\setminus\bar{J}} w + w$$
$$\Rightarrow \sum_{j\in J_t\setminus\bar{J}} x_{j1} \leq |J_t \setminus \bar{J}|w + 1 \tag{22}$$

Case 5. $X = \{d_1, [p_j]_{j\in\bar{J}}, d_2\}$: For this case, $\delta^+(X) = \{(p_j, q)\ \forall j \in \bar{J}\} \cup \{(d_1, p_j)\ \forall j \in J_t \setminus \bar{J}\}$, $\delta^-(X) = \{(p_j, d_2)\ \forall j \in J_t \setminus \bar{J}\} \cup (q, d_2)$. (17) $\Rightarrow$

$$\sum_{j\in\bar{J}} \ell(p_j, q) + \sum_{j\in J_t\setminus\bar{J}} \ell(d_1, p_j) \leq \sum_{j\in J_t\setminus\bar{J}} u(p_j, d_2) + u(q, d_2)$$
$$\Rightarrow 0 \leq \sum_{j\in J_t\setminus\bar{J}} w + w$$
$$\Rightarrow w \geq 0 \tag{23}$$

Case 6. $X = \{[p_j]_{j\in\bar{J}}, q, d_2\}$: For this case, $\delta^+(X) = (d_2, d_1)$, $\delta^-(X) = \{(p_j, d_2)\ \forall j \in J_t \setminus \bar{J}\} \cup \{(p_j, q)\ \forall j \in J_t \setminus \bar{J}\} \cup \{(d_1, p_j)\ \forall j \in \bar{J}\}$. (17) $\Rightarrow$

$$\ell(d_2, d_1) \leq \sum_{j\in J_t\setminus\bar{J}} u(p_j, d_2) + \sum_{j\in J_t\setminus\bar{J}} u(p_j, q) + \sum_{j\in\bar{J}} u(d_1, p_j)$$

$$\Rightarrow -1 + w + \sum_{j\in J_t} x_{j1} \le \sum_{j\in J_t\setminus\bar{J}} w + \sum_{j\in J_t\setminus\bar{J}} x_{j2} + \sum_{j\in\bar{J}} x_{j1}$$
$$\Rightarrow \sum_{j\in J_t\setminus\bar{J}} (x_{j1} - x_{j2}) \le (|J_t\setminus\bar{J}|-1)w + 1 \tag{24}$$

Case 7. $X = \{d_1, [p_j]_{j\in\bar{J}}, q\}$: For this case, $\delta^+(X) = \{(p_j, d_2)\ \ \forall j \in \bar{J}\} \cup \{(d_1, p_j)\ \ \forall j \in J_t\setminus\bar{J}\} \cup (q, d_2)$, $\delta^-(X) = (d_2, d_1) \cup \{(p_j, q)\ \ \forall j \in J_t\setminus\bar{J}\}$. (17) $\Rightarrow$

$$\sum_{j\in\bar{J}} \ell(p_j, d_2) + \sum_{j\in J_t\setminus\bar{J}} \ell(d_1, p_j) + \ell(q, d_2) \le \sum_{j\in J_t\setminus\bar{J}} u(p_j, q) + u(d_2, d_1)$$
$$\Rightarrow \sum_{j\in\bar{J}} (x_{j1} - x_{j2}) - 1 + w + \sum_{j\in J_t} x_{j2} \le \sum_{j\in J_t\setminus\bar{J}} x_{j2} + w$$
$$\Rightarrow \sum_{j\in\bar{J}} x_{j1} \le 1 \tag{25}$$

Case 8. $X = \{d_1, [p_j]_{j\in\bar{J}}, q, d_2\}$: For this case, $\delta^+(X) = \{(d_1, p_j)\ \ \forall j \in J_t\setminus\bar{J}\}$, $\delta^-(X) = \{(p_j, q)\ \ \forall j \in J_t\setminus\bar{J}\} \cup \{(p_j, d_2)\ \ \forall j \in J_t\setminus\bar{J}\}$. (17) $\Rightarrow$

$$\sum_{j\in J_t\setminus\bar{J}} \ell(d_1, p_j) \le \sum_{j\in J_t\setminus\bar{J}} u(p_j, q) + \sum_{j\in J_t\setminus\bar{J}} u(p_j, d_2)$$
$$\Rightarrow \sum_{j\in J_t\setminus\bar{J}} x_{j2} + \sum_{j\in J_t\setminus\bar{J}} w \ge 0 \tag{26}$$

Cases 1-8 cover all possible $X \subseteq \bar{V}$ since $\bar{J}$ can be empty. Non-dominated constraints among (19)-(26) are:

$$\sum_{j\in\bar{J}} (x_{j1} - x_{j2}) \le w \qquad \forall \bar{J} \subseteq J_t, \tag{27a}$$
$$\sum_{j\in J_t} x_{j1} \le 1,\ 0 \le w \le 1,\ x_{j2} \ge 0. \tag{27b}$$

By definition, $\ell(a, b) \le u(a, b)\ \ \forall (a, b) \in \bar{E}$. From this condition, we obtain:

$$\sum_{j\in J_t} x_{j1} \le 1,\ \sum_{j\in J_t} x_{j2} \le 1, \tag{28a}$$
$$x_{j1} \ge 0,\ x_{j2} \ge 0 \qquad \forall j \in J_t. \tag{28b}$$

From Lemma 1, there exists a circulation on $G(\bar{V}, \bar{E})$ if and only if (27)-(28) are feasible. Therefore, $\mathcal{V}_{it} \ne \emptyset$ if and only if both (27) and (28) are feasible. Combining (27)-(28) and substituting $x_{j1} = x_{ijt}$, $x_{j2} = x_{ij(t+1)}$, and $w = w_{it}$, we obtain

$$\sum_{j\in\bar{J}} (x_{ijt} - x_{ij(t+1)}) \le w_{it} \qquad \forall \bar{J} \subseteq J_t, \tag{29a}$$

$$\sum_{j\in J_t} x_{ijt} \le 1,\ \sum_{j\in J_t} x_{ij(t+1)} \le 1, \tag{29b}$$

$$x_{ijt} \ge 0,\ x_{ij(t+1)} \ge 0,\ 0 \le w_{it} \le 1 \tag{29c}$$

which coincides exactly with the constraint set defining $\tilde{\mathcal{Q}}^L_{it}$. Thus, for every $(w_{it}, \mathbf{x}_{it}, \mathbf{x}_{i(t+1)}) \in \tilde{\mathcal{Q}}^L_{it}$, as $\mathcal{V}_{it} \neq \emptyset$, $\exists(\mathbf{x}^1_{it}, \mathbf{x}^2_{i(t+1)})$ such that $(w_{it}, \mathbf{x}_{it}, \mathbf{x}_{i(t+1)}, \mathbf{x}^1_{it}, \mathbf{x}^2_{i(t+1)}) \in \mathcal{V}_{it}$. As a result, $\tilde{\mathcal{Q}}^L_{it} = \text{Proj}_{(w_{it}, \mathbf{x}_{it}, \mathbf{x}_{i(t+1)})}\, \mathcal{V}_{it}$. □

Proof of Proposition 4: For some $i \in I$, $t \in T \setminus \{|T|\}$, consider the inequalities (5):

$$w_{it} \ge \sum_{j\in\bar{J}} \left(x_{ijt} - x_{ij(t+1)}\right) \qquad \forall \bar{J} \subseteq J_t \tag{30a}$$

$$\Rightarrow w_{it} \ge \max_{\bar{J}\subseteq J_t} \sum_{j\in\bar{J}} \left(x_{ijt} - x_{ij(t+1)}\right) \tag{30b}$$

$$\Rightarrow w_{it} \ge \eta_{it} = \max \sum_{j\in J_t} \left(x_{ijt} - x_{ij(t+1)}\right) y_j \tag{30c}$$

$$\text{s.t. } 0 \le y_j \le 1 \qquad \forall j \in J_t. \tag{30d}$$

Here, $y_j \ge 0$ due to $w_{it} \ge 0$. Dualizing the LP defining η_{it} we get:

$$\eta_{it} = \min \sum_{j\in J_t} \beta_{ijt} \tag{31a}$$

$$\text{s.t. } \beta_{ijt} \ge x_{ijt} - x_{ij(t+1)} \qquad \forall j \in J_t, \tag{31b}$$

$$\beta_{ijt} \ge 0 \qquad \forall j \in J_t. \tag{31c}$$

Combining (30c), (30d) and (31), we get (9). □

Proof of Proposition 5: Given a first-stage solution $\mathbf{r}$, assume that there exists an optimal second-stage solution $(\mathbf{x}^*, \mathbf{w}^*, \bar{\mathbf{w}}^*)$ where (10) is violated. Since $c^h > 0$, we may assume that $\mathbf{w}^*$ and $\bar{\mathbf{w}}^*$ take the smallest values permitted by (2c) and (2d). Then, there exists an $s \in S$, $i \in I_s$, $t < T^e_s$ with $w^*_{it} = 1$, and an OR $j \in J_t$ with $x^*_{ijt} = 1$ and $x^*_{ij(t+1)} = 0$. Without loss of generality, let t be the earliest period where (10) is violated for any CRNA. Let $\varepsilon_{jt} = \min\{\, \theta \ge t : j \notin J_\theta \,\}$ be the last period of the surgery ongoing in OR j in period t, and set $\tau = \min\{T^e_s, \varepsilon_{jt}\}$.

We construct another solution $\mathbf{x}'$ from $\mathbf{x}^*$ as follows. For every $\theta \in \{t+1, \ldots, \tau\}$ with $x^*_{ij\theta} = 0$, we set

- $x'_{ij\theta} = 1$,

- $x'_{i\tilde{j}\theta} = 0$ for every $\tilde{j} \in J \setminus \{j\}$ with $x^*_{i\tilde{j}\theta} = 1$,
- $x'_{\tilde{i}j\theta} = 0$ for every $\tilde{i} \in I \cup \{i_d\}$ with $x^*_{\tilde{i}j\theta} = 1$,
- $x'_{\tilde{i}\tilde{j}\theta} = 1$ for every $\tilde{i} \in I \cup \{i_d\}$ and $\tilde{j} \in J \setminus \{j\}$ with $x^*_{\tilde{i}j\theta} = x^*_{i\tilde{j}\theta} = 1$.

All remaining components of $\mathbf{x}'$ are the same as those of $\mathbf{x}^*$, and $\mathbf{w}'$ and $\bar{\mathbf{w}}'$ take the smallest values permitted by (2c) and (2d) for $\mathbf{x}'$. $(\mathbf{x}', \mathbf{w}', \bar{\mathbf{w}}')$ is feasible for $SS_{\mathbf{r},\omega}$. Indeed, as $\mathbf{x}'$ covers the same ORs as $\mathbf{x}^*$ in each time period, (2b) and (2e) remain satisfied, while (2c) and (2d) hold by construction. Next, we show that $(\mathbf{x}', \mathbf{w}', \bar{\mathbf{w}}')$ incurs no more under-staffed time periods or handovers than $(\mathbf{x}^*, \mathbf{w}^*, \bar{\mathbf{w}}^*)$ and is therefore also optimal.

First, we compare the number of under-staffed time periods under $(\mathbf{x}^*, \mathbf{w}^*, \bar{\mathbf{w}}^*)$ and $(\mathbf{x}', \mathbf{w}', \bar{\mathbf{w}}')$. Since $\mathbf{x}'$ and $\mathbf{x}^*$ coincide in every period outside $\{t+1, \ldots, \tau\}$,

$$\sum_{\tilde{j} \in J} x'_{i_d\tilde{j}\theta} = \sum_{\tilde{j} \in J} x^*_{i_d\tilde{j}\theta} \qquad \forall \theta \in T \setminus \{t+1, \ldots, \tau\}. \tag{32}$$

Now consider a period $\theta \in \{t+1, \ldots, \tau\}$. Under $\mathbf{x}'$, CRNA i_d is not assigned to OR j in period θ, that is, $x'_{i_dj\theta} = 0$. Moreover, if CRNA i_d is assigned to j and CRNA i is assigned to some $\tilde{j} \in J \setminus \{j\}$ under $\mathbf{x}^*$, then CRNA i_d is assigned to $\tilde{j}$ under $\mathbf{x}'$, and all other assignments of CRNA i_d in period θ are the same under $\mathbf{x}'$ and $\mathbf{x}^*$. That is, $x'_{i_d\tilde{j}\theta} = x^*_{i_d\tilde{j}\theta} + x^*_{i_dj\theta}\, x^*_{i\tilde{j}\theta}$ for every $\tilde{j} \in J \setminus \{j\}$, where the product $x^*_{i_dj\theta}\, x^*_{i\tilde{j}\theta}$ equals 1 exactly when CRNA i_d is assigned to j and CRNA i is assigned to $\tilde{j}$ under $\mathbf{x}^*$. When this product equals 1, $x^*_{i_d\tilde{j}\theta} = 0$ by (2e), so the two terms on the right-hand side cannot both equal to 1. Summing these equalities over $\tilde{j} \in J \setminus \{j\}$ and using $x'_{i_dj\theta} = 0$ for OR j, we obtain, for every $\theta \in \{t+1, \ldots, \tau\}$,

$$\begin{aligned} \sum_{\tilde{j} \in J} x'_{i_d\tilde{j}\theta} &= \sum_{\tilde{j} \in J \setminus \{j\}} x^*_{i_d\tilde{j}\theta} + x^*_{i_dj\theta} \sum_{\tilde{j} \in J \setminus \{j\}} x^*_{i\tilde{j}\theta} \\ &\leq \sum_{\tilde{j} \in J \setminus \{j\}} x^*_{i_d\tilde{j}\theta} + x^*_{i_dj\theta} \\ &= \sum_{\tilde{j} \in J} x^*_{i_d\tilde{j}\theta} \end{aligned} \tag{33}$$

where the inequality holds since $\sum_{\tilde{j} \in J \setminus \{j\}} x^*_{i\tilde{j}\theta} \leq 1$ by (2b). Summing (32) and (33) over $\theta \in T$ yields

$$\sum_{\tilde{j} \in J} \sum_{\theta \in T} x'_{i_d\tilde{j}\theta} \leq \sum_{\tilde{j} \in J} \sum_{\theta \in T} x^*_{i_d\tilde{j}\theta}. \tag{34}$$

This shows that the number of under-staffed time periods under $(\mathbf{x}', \mathbf{w}', \bar{\mathbf{w}}')$ does not exceed that under $(\mathbf{x}^*, \mathbf{w}^*, \bar{\mathbf{w}}^*)$.

Next, we compare the number of handovers under $(\mathbf{x}^*, \mathbf{w}^*, \bar{\mathbf{w}}^*)$ and $(\mathbf{x}', \mathbf{w}', \bar{\mathbf{w}}')$. For each $\theta \in T \setminus \{|T|\}$, the variables $\mathbf{w}$ and $\bar{\mathbf{w}}$ are determined by the assignments in consecutive time periods. Since $\mathbf{x}'$ and $\mathbf{x}^*$ coincide in periods $\theta \in T \setminus \{t+1, \ldots, \tau\}$, it follows that

$$\sum_{\tilde{\imath} \in I} (w'_{\tilde{\imath}\theta} + \bar{w}'_{\tilde{\imath}\theta}) = \sum_{\tilde{\imath} \in I} (w^*_{\tilde{\imath}\theta} + \bar{w}^*_{\tilde{\imath}\theta}) \qquad \forall \theta \in T \setminus \{|T|\} : \theta < t \text{ or } \theta > \tau. \tag{35}$$

Now consider a period $\theta \in \{t, \ldots, \tau\} \setminus \{|T|\}$. We say that the assigned CRNA of an OR $\tilde{\jmath} \in J_\theta$ changes at the end of period θ if different CRNAs are assigned to $\tilde{\jmath}$ in periods θ and $\theta+1$. By (2b) and (2e), and since $\mathbf{w}$ and $\bar{\mathbf{w}}$ take the smallest values permitted by (2c) and (2d), $\sum_{\tilde{\imath} \in I}(w_{\tilde{\imath}\theta} + \bar{w}_{\tilde{\imath}\theta})$ equals the number of ORs in J_θ whose assigned CRNA changes at the end of period θ. In each period $\theta \in \{t+1, \ldots, \tau\}$, $\mathbf{x}'$ and $\mathbf{x}^*$ differ only in the assignments to OR j and to $\tilde{\jmath} \in J \setminus \{j\}$ with $x^*_{i\tilde{\jmath}\theta} = 1$. Hence, it suffices to compare handovers in OR j and in the ORs to which CRNA i is assigned under $\mathbf{x}^*$ in each $\theta \in \{t, \ldots, \tau\} \setminus \{|T|\}$. We consider three cases: $\theta = t$, $t < \theta < \tau$, and $\theta = \tau$. In the cases below, unless stated otherwise, all changes of assigned CRNAs and all handovers are at the end of period θ.

Case 1: $\theta = t$. Since $x^*_{ijt} = 1$ and $x^*_{ij(t+1)} = 0$, the assigned CRNA of OR $j \in J_t$ changes under $\mathbf{x}^*$, whereas $x'_{ijt} = x'_{ij(t+1)} = 1$ implies that it does not change under $\mathbf{x}'$. Moreover, any $\tilde{\jmath} \in J_t \setminus \{j\}$ with $x^*_{i\tilde{\jmath}(t+1)} = 1$ satisfies $x^*_{i\tilde{\jmath}t} = 0$ (by (2b), as $x^*_{ijt} = 1$), so its assigned CRNA changes under $\mathbf{x}^*$, and OR $\tilde{\jmath}$ has no more handovers under $\mathbf{x}'$ than under $\mathbf{x}^*$. This implies

$$\sum_{\tilde{\imath} \in I} (w'_{\tilde{\imath}t} + \bar{w}'_{\tilde{\imath}t}) \le \sum_{\tilde{\imath} \in I} (w^*_{\tilde{\imath}t} + \bar{w}^*_{\tilde{\imath}t}) - 1. \tag{36}$$

Case 2: $t < \theta < \tau$. Here, $j \in J_\theta$, since $\theta < \tau \le \varepsilon_{jt}$. Since $x'_{ij\theta} = x'_{ij(\theta+1)} = 1$, the assigned CRNA of OR j does not change under $\mathbf{x}'$, and hence OR j has no more handovers under $\mathbf{x}'$ than under $\mathbf{x}^*$ By construction, apart from OR j, the only ORs whose assigned CRNAs in periods θ and $\theta+1$ can differ between $\mathbf{x}'$ and $\mathbf{x}^*$ are the ones in which CRNA i is assigned under $\mathbf{x}^*$ in period θ or $\theta+1$. Consider such an OR $\tilde{\jmath} \in J_\theta \setminus \{j\}$ with $x^*_{i\tilde{\jmath}\theta} + x^*_{i\tilde{\jmath}(\theta+1)} \ge 1$. If $x^*_{i\tilde{\jmath}\theta} + x^*_{i\tilde{\jmath}(\theta+1)} = 1$, then CRNA i is assigned to $\tilde{\jmath}$ under $\mathbf{x}^*$ in exactly one of the periods θ and $\theta+1$. Hence, the assigned CRNA of OR $\tilde{\jmath}$ changes under $\mathbf{x}^*$, and OR $\tilde{\jmath}$ has no more handovers under $\mathbf{x}'$ than under $\mathbf{x}^*$. If $x^*_{i\tilde{\jmath}\theta} + x^*_{i\tilde{\jmath}(\theta+1)} = 2$, then the assigned CRNA of OR $\tilde{\jmath}$ does not change under $\mathbf{x}^*$. Under $\mathbf{x}'$, $\tilde{\jmath}$ is assigned, in periods θ and $\theta+1$, the CRNAs assigned to j under $\mathbf{x}^*$. Hence, the assigned CRNA of OR $\tilde{\jmath}$ changes under $\mathbf{x}'$ only if that of OR j changes under $\mathbf{x}^*$.

Since the assigned CRNA of OR j does not changed under $\mathbf{x}'$, ORs j and $\tilde{j}$ together have no more handovers under $\mathbf{x}'$ than under $\mathbf{x}^*$ Therefore,

$$\sum_{\tilde{i}\in I}(w'_{\tilde{i}\theta}+\bar{w}'_{\tilde{i}\theta}) \le \sum_{\tilde{i}\in I}(w^*_{\tilde{i}\theta}+\bar{w}^*_{\tilde{i}\theta}) \qquad \forall \theta \in \{t+1,\dots,\tau-1\}. \tag{37}$$

Case 3: $\theta=\tau<|T|$. In periods τ and $\tau+1$, $\mathbf{x}'$ and $\mathbf{x}^*$ differ only in period τ, and only in ORs j and $\tilde{j}\in J\setminus\{j\}$ with $x^*_{i\tilde{j}\tau}=1$. We consider the following sub-cases.

Case 3a: $\tau=\varepsilon_{jt}$. This implies $j\notin J_\tau$ and therefore, no handover in OR j is counted under either $\mathbf{x}^*$ or $\mathbf{x}'$. The assigned CRNA of OR $\tilde{j}\in J_\tau$ will change under $\mathbf{x}'$ but will not change under $\mathbf{x}^*$ only if $x^*_{i\tilde{j}\tau}=x^*_{i\tilde{j}(\tau+1)}=1$.

Case 3b: $\tau=T^e_s<\varepsilon_{jt}$. This implies $j\in J_\tau$. Any $\tilde{j}\in J_\tau\setminus\{j\}$ with $x^*_{i\tilde{j}\tau}=1$ satisfies $x^*_{i\tilde{j}(\tau+1)}=0$ as the shift of CRNA i ends in period τ. Therefore, the assigned CRNA of OR $\tilde{j}$ changes under $\mathbf{x}^*$, and OR $\tilde{j}$ has no more handovers under $\mathbf{x}'$ than under $\mathbf{x}^*$. The assigned CRNA of OR j changes under $\mathbf{x}'$ but will not change under $\mathbf{x}^*$ only if $x^*_{\tilde{i}j\tau}=x^*_{\tilde{i}j(\tau+1)}=1$, for some $\tilde{i}\in I\cup\{i_d\}\setminus\{i\}$. Thus, $w'_{i\tau}=1$, a handover from CRNA i at the end of its shift, which (10) permits.

In both sub-cases, the CRNA assigned at the end of period τ may change under $\mathbf{x}'$ but remain unchanged under $\mathbf{x}^*$ for at most one OR. Therefore,

$$\sum_{\tilde{i}\in I}(w'_{\tilde{i}\tau}+\bar{w}'_{\tilde{i}\tau}) \le \sum_{\tilde{i}\in I}(w^*_{\tilde{i}\tau}+\bar{w}^*_{\tilde{i}\tau})+1. \tag{38}$$

Adding (35), (36), (37), and (38) over their respective periods gives

$$\sum_{\theta\in T\setminus\{|T|\}}\sum_{\tilde{i}\in I}(w'_{\tilde{i}\theta}+\bar{w}'_{\tilde{i}\theta}) \le \sum_{\theta\in T\setminus\{|T|\}}\sum_{\tilde{i}\in I}(w^*_{\tilde{i}\theta}+\bar{w}^*_{\tilde{i}\theta}). \tag{39}$$

By (34), (39), and (2a), the second-stage objective value of $(\mathbf{x}',\mathbf{w}',\bar{\mathbf{w}}')$ is no greater than that of $(\mathbf{x}^*,\mathbf{w}^*,\bar{\mathbf{w}}^*)$. Hence, $(\mathbf{x}',\mathbf{w}',\bar{\mathbf{w}}')$ is also optimal. Moreover, constructing $(\mathbf{x}',\mathbf{w}',\bar{\mathbf{w}}')$ eliminates the violation of (10) at (i,t), although violations may remain in periods after t. Therefore, repeatedly applying this construction to the earliest remaining violation eliminates all violations in finitely many steps, yielding an optimal solution of $SS_{\mathbf{r},\omega}$ that satisfies (10). □

Appendix C: Surgery Data

Table 6 Summary of 353-Day surgery data

Specialty	Duration average (min)	Duration standard deviation (min)	Case mix (%)
Dentistry	197	58	1.77
Gastroenterology	106	71	0.28
General	100	59	1.16
Gynecology	131	79	5.22
Gynecology Oncology	78	0	0.01
Interventional Radiology	79	5	0.01
Neurology	65	12	0.14
Obstetrics	80	25	0.01
Ophthalmology	71	48	23.42
Oral Surgery	151	68	0.05
Orthopedics	147	77	14.59
Otolaryngology	163	115	13.05
Pain	91	52	1.53
Pediatric Gastroenterology	75	2	0.01
Pediatric General	139	45	0.05
Pediatric Ophthalmology	98	37	3.82
Pediatric Orthopedics	140	52	0.17
Pediatric Urology	91	49	1.06
Plastics	132	87	1.84
Podiatry	156	104	1.48
Pediatric ENT	108	87	3.95
Pediatric Neurology	62	37	0.07
Surgical Oncology	148	84	2.90
Urology	76	50	23.40

Table 7 Surgery and Shift Data

	Day 1	Day 2	Day 3
Number of surgeries	56	41	37
Number of open ORs	9	9	9
Number of available CRNAs:			
Shift 1: 7 a.m.- 3 p.m.	3	7	3
Shift 2: 7 a.m.- 5 p.m.	5	6	7
Shift 3: 7 a.m.- 7 p.m.	5	1	3
Shift 4: 7 a.m.- 9 p.m.	2	0	1

Table 8 Surgery Scheduling Details - Day 1

Specialty		(OR, starting time period)
Type	No of Surgeries	
Ophthalmology	20	(7, 1), (4, 1), (4, 3), (7, 4), (7, 7), (4, 8), (4, 9), (7, 10), (7, 13), (7, 16), (7, 19), (4, 21), (7, 22), (7, 25), (4, 27), (7, 28), (4, 30), (7, 31), (4, 33), (7, 34)
Orthopedics	11	(5, 1),(2, 1), (6, 1), (2, 4), (5, 8), (2, 8), (2, 14), (2, 17), (5, 19), (5, 26), (5, 32)
Otolaryngology	4	(3, 1), (3, 4), (1, 11), (3, 15)
Pediatric ENT	6	(1, 1), (1, 4), (1, 6), (1, 21), (1, 27), (1, 33)
Urology	15	(9, 2), (9, 6), (8, 7), (9, 11), (8, 11), (8, 14), (9, 15), (8, 16), (8, 18), (9, 19), (8, 24), (9, 27), (8, 29), (9, 33), (9, 39)

Table 9 Surgery Scheduling Details - Day 2

Specialty		(OR, starting time period)
Type	No of Surgeries	
Gynecology	7	(2, 1), (2, 10), (2, 16), (2, 20), (2, 24), (2, 28), (2, 33)
Ophthalmology	9	(7, 5), (7, 7), (7, 11), (7, 16), (7, 20), (7, 23), (7, 27), (5, 28), (7,31)
Oral Surgery	1	(3, 33)
Orthopedics	9	(6, 1), (4, 1), (5, 1), (4, 10), (6, 12), (5, 18), (4, 19), (6, 25), (6, 31)
Otolaryngology	2	(3, 1), (3, 14)
Pediatric Urology	3	(8, 6), (8, 12), (8, 18)
Pediatric ENT	3	(1, 1), (1, 16), (1, 24)
Urology	7	(9, 1), (9, 7), (9, 13), (9, 19), (9, 25), (9, 31), (9, 35)

Table 10 Surgery Scheduling Details - Day 3

Specialty		(OR, starting time period)
Type	No of Surgeries	
Ophthalmology	12	(7, 1), (4, 1), (7, 3), (7, 6), (4, 8), (7, 9), (7, 12), (4, 14), (7, 15), (4, 20), (4, 26), (4, 31)
Orthopedics	7	(5, 1), (6, 1), (6, 4), (6, 9), (6, 14), (5, 21), (1, 33)
Otolaryngology	4	(3, 1), (1, 1), (3, 9), (1, 12)
Pediatric Ophthalmology	3	(7, 18),(7, 24), (7, 29)
Surgical Oncology	5	(2, 1), (2, 8), (2, 16), (2, 23), (2, 31)
Urology	6	(9, 9), (6, 23), (9, 25), (8, 27), (6, 30), (9, 3)

Appendix D: $SS_{\mathbf{r},\omega}$ with overtime

Let c^o be the per-period cost of CRNA overtime and $\{T_s^b, \cdots, T_s^e\}$ denote the time periods covered by shift s. Let $\zeta_{it}(\omega)$ be a binary variable that equals 1 if time period t is the last period after the shift end in which CRNA i is assigned to an OR under scenario ω, and 0 otherwise. Using these notations, $SS_{\mathbf{r},\omega}$ with CRNA overtime is given by:

$$\text{Min} \sum_{i\in I}\sum_{t\in T} c^h w_{it}(\omega) + \sum_{i\in I}\sum_{t\in T} c^h \bar{w}_{it}(\omega) + \sum_{j\in J}\sum_{t\in T} c^u x_{i_d jt}(\omega) + \sum_{s\in S}\sum_{i\in I_s}\sum_{t=T_s^e+1}^{|T|} (t-T_s^e)c^o \zeta_{it}(\omega) \tag{40a}$$

s.t. (2c), (2d), (2e)

$$\sum_{j\in J} x_{ijt}(\omega) \le r_i \qquad \forall s\in S, i\in I_s, t\in T, \tag{40b}$$

$$x_{ijt}(\omega) = 0 \qquad \forall s\in S, i\in I_s, j\in J, t\in\{1,\cdots,T_s^b-1\}, \tag{40c}$$

$$\sum_{\tau=t}^{|T|} \zeta_{i\tau}(\omega) \ge x_{ijt}(\omega) \qquad \forall s\in S, i\in I_s, j\in J, t\in\{T_s^e+1,\cdots,|T|\}, \tag{40d}$$

$$\boldsymbol{\zeta}(\omega) \in \mathbb{B}^{\sum_{s\in S}|I_s|(|T|-T_s^e)}, \tag{40e}$$

$$\mathbf{x}(\omega) \in \mathbb{B}^{(|I|+1)\times|J|\times|T|}, \ \ \mathbf{w}(\omega), \bar{\mathbf{w}}(\omega) \in \mathbb{B}^{(|I|)\times(|T|-1)}. \tag{40f}$$

(40b) ensures that CRNAs are allocated to ORs only if they are called. (40c) prevents CRNAs from being allocated to an OR before their shift begins, while (40d) tracks the last time period in which CRNAs are allocated to an OR after their shift ends. Lastly, the first three

terms of the objective function (40a) are the same as (2a) while the last term models the total overtime cost. The valid inequalities (5) remain valid for (40), while the supervalid equalities (10) take the form $w_{it}(\omega) = 0$ for $t < T_s^e$ and $w_{it}(\omega) \leq \zeta_{it}(\omega)$ for $t > T_s^e$, for all $s \in S$ and $i \in I_s$.

Appendix E: Additional Computational Results

Table 11 Average (max) optimality gap (%) and runtime (s), $|\Omega| = 500$.

		Optimality gap (%)			
Case	ψ—χ	ILS-L	ILS-L$_{(5)}$	ILS-L$_{(10)}$	ILS-L$_{(5,10)}$
1	30—5	0.87 (2.90)	0.35 (1.00)	0.17 (0.82)	0.43 (1.00)
2	30—10	0.21 (0.98)	0.51 (0.94)	0.31 (0.99)	0.47 (0.87)
3	30—20	1.18 (10.66)	0.70 (1.00)	0.18 (0.57)	0.73 (1.00)
4	40—5	0.64 (4.32)	0.20 (0.98)	0.83 (4.32)	0.35 (0.99)
5	40—10	2.08 (7.23)	0.20 (0.50)	0.24 (0.65)	0.33 (0.93)
6	40—20	0.33 (0.95)	0.68 (1.00)	0.27 (0.99)	0.53 (1.00)
7	50—5	0.51 (2.98)	0.19 (0.90)	0.39 (0.84)	0.41 (1.00)
8	50—10	2.45 (7.36)	0.18 (0.39)	1.12 (7.20)	0.30 (0.87)
9	50—20	2.39 (7.32)	0.64 (0.99)	0.46 (1.11)	0.49 (0.88)
		Runtime (s)			
Case	ψ—χ	ILS-L	ILS-L$_{(5)}$	ILS-L$_{(10)}$	ILS-L$_{(5,10)}$
1	30—5	2805 (3677)	1314 (2170)	2035 (3172)	1049 (1662)
2	30—10	2488 (3471)	1144 (2575)	2002 (3359)	930 (1807)
3	30—20	1637 (3610)	868 (1320)	1486 (2251)	720 (1201)
4	40—5	2455 (3613)	1258 (2185)	1958 (3899)	1034 (1778)
5	40—10	2849 (3910)	1139 (2541)	2128 (3319)	910 (1923)
6	40—20	2011 (3220)	869 (1324)	1897 (3262)	759 (1198)
7	50—5	2154 (3607)	1097 (2218)	1613 (2330)	1021 (1593)
8	50—10	2927 (3826)	969 (1655)	2200 (3703)	829 (1199)
9	50—20	2746 (3848)	843 (1208)	2250 (3721)	865 (1637)

Table 12 Average (max) optimality gap (%) and runtime (s), $|\Omega|=1000$.

Case	ψ—χ	Optimality gap (%)			
		ILS-L	ILS-L$_{(5)}$	ILS-L$_{(10)}$	ILS-L$_{(5,10)}$
1	30—5	6.44 (14.36)	1.03 (6.95)	2.42 (8.82)	0.42 (0.94)
2	30—10	17.36 (94.18)	12.38 (93.35)	2.88 (9.02)	0.51 (0.98)
3	30—20	2.40 (10.04)	4.85 (19.82)	1.91 (8.03)	0.73 (1.00)
4	40—5	6.24 (16.05)	1.03 (6.17)	1.73 (6.19)	0.38 (0.75)
5	40—10	8.83 (17.53)	1.07 (6.65)	4.26 (12.54)	0.41 (0.97)
6	40—20	5.35 (9.98)	4.89 (19.83)	5.19 (17.48)	0.68 (1.00)
7	50—5	4.14 (9.57)	0.39 (0.89)	1.40 (4.05)	0.60 (0.99)
8	50—10	11.20 (25.50)	1.51 (10.09)	3.91 (10.05)	0.19 (0.44)
9	50—20	8.99 (14.39)	2.87 (20.33)	4.71 (16.97)	0.53 (1.00)
		Runtime (s)			
Case	ψ—χ	ILS-L	ILS-L$_{(5)}$	ILS-L$_{(10)}$	ILS-L$_{(5,10)}$
1	30—5	3583 (4522)	2322 (3807)	3486 (4164)	2067 (3153)
2	30—10	3537 (4003)	2249 (3818)	3373 (4310)	1872 (2897)
3	30—20	2827 (3802)	1998 (3970)	2705 (3817)	1688 (3382)
4	40—5	3527 (4699)	2170 (3936)	3343 (4116)	1864 (2827)
5	40—10	3666 (4124)	1903 (3714)	3422 (3857)	1890 (2447)
6	40—20	3318 (4011)	2120 (4196)	3030 (3890)	1746 (3003)
7	50—5	3228 (3864)	2008 (3197)	3087 (3836)	2029 (3205)
8	50—10	3765 (4195)	2200 (3808)	3400 (3795)	1938 (3280)
9	50—20	3898 (4647)	2124 (4130)	3353 (3830)	1697 (3254)

Table 13 Comparison of Stochastic Solution and Mean Value Solution for $|\Omega|=1000$.

Case	ψ—χ	VSS	κ_{HO}	κ_{US}	κ_{SC}	κ_{S_1}	κ_{S_2}	κ_{S_3}	κ_{S_4}
1	30—5	2.90	-11.58	10.17	-2.33	44.44	-40.00	0.00	0.00
2	30—10	5.12	4.10	10.43	-2.33	44.44	-40.00	0.00	0.00
3	30—20	5.56	10.82	8.90	-5.26	33.33	-62.22	0.00	0.00
4	40—5	2.58	-12.36	8.01	-2.07	38.89	-34.44	0.00	0.00
5	40—10	4.98	-1.72	10.82	-2.33	44.44	-40.00	0.00	0.00
6	40—20	6.59	9.64	9.25	-2.54	55.56	-51.11	0.00	0.00
7	50—5	2.51	-9.90	7.34	-2.07	38.89	-34.44	0.00	0.00
8	50—10	4.75	-5.90	10.48	-2.33	44.44	-40.00	0.00	0.00
9	50—20	6.61	6.80	10.34	-3.57	50.00	-51.11	0.00	0.00